

AD-A054 726

SYSTEMS EXPLORATION INC SAN DIEGO CA
HF CHANNEL SIMULATOR FOR WIDEBAND SIGNALS. A MATHEMATICAL MODEL--ETC(U)
MAR 78 R LUGANNANI, H C BOOKER, L E HOFF

F/G 17/2

N00123-76-C-1090

UNCLASSIFIED

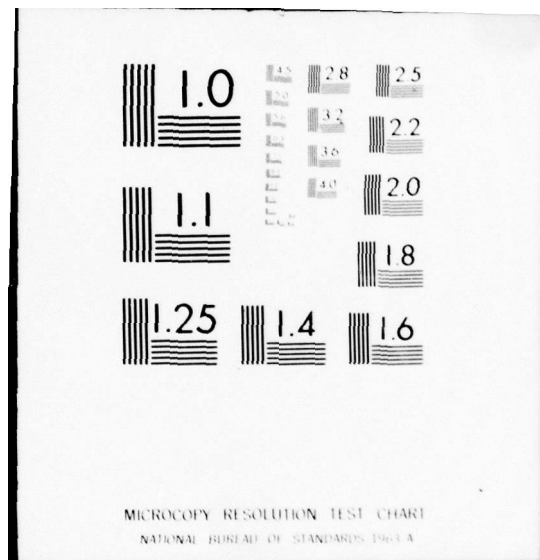
NOSC-TR-208

ALL

1 of 2
AD
A054726

NOSC





FOR FURTHER TRAN

12

ADA 054726

NOSC

NOSC

NOSC TR 208

Technical Report 208

HF CHANNEL SIMULATOR FOR WIDEBAND SIGNALS

A Mathematical Model and Computer Program for 100-kHz Bandwidth HF Channels

R Lugannani and HG Booker
LE Hoff (Contract Monitor)
31 March 1978

Final Report: February 1977 - October 1977

Prepared for
Naval Electronic Systems Command

AD No. _____
DDC FILE COPY

APPROVED FOR PUBLIC RELEASE; DISTRIBUTION UNLIMITED

NAVAL OCEAN SYSTEMS CENTER
SAN DIEGO, CALIFORNIA 92152

DDC
RECEIVED
JUN 8 1978
B



NAVAL OCEAN SYSTEMS CENTER, SAN DIEGO, CA 92152

AN ACTIVITY OF THE NAVAL MATERIAL COMMAND
RR GAVAZZI, CAPT, USN

Commander

HL BLOOD

Technical Director

ADMINISTRATIVE INFORMATION

Work was performed under contract N000123-76-C-1090/SEI-C-020 by Systems Exploration, Inc. for Intra-Task Force/SS Com Branch, Communications Systems and Technology Department, NOSC.

This work was performed as part of NAVELEX's Skywave Communications Task, a 6.2 Block-Funded Program. This report covers work from February 1977 to October 1977 and was approved for publication January 1978.

Released by
CA NELSON, Head
Surface/Shore Systems Division

Under authority of
RO EASTMAN, Head
Communications Systems and
Technology Department

UNCLASSIFIED

SECURITY CLASSIFICATION OF THIS PAGE (When Data Entered)

19 REPORT DOCUMENTATION PAGE		READ INSTRUCTIONS BEFORE COMPLETING FORM
1. REPORT NUMBER 18 NO SC TR-298	2. GOVT ACCESSION NO.	3. RECIPIENT'S CATALOG NUMBER
6 HF Channel Simulator for Wideband Signals. A Mathematical Model and Computer Program for 100-kHz Bandwidth HF Channels.	9	5. TYPE OF REPORT & PERIOD COVERED Final Report February 1977 - October 1977
		6. PERFORMING ORG. REPORT NUMBER
10 R. LUGANNANI, HC BOOKER LE Hoff (Contract Monitor)	15	8. CONTRACT OR GRANT NUMBER(s) N000123-76-C-1090^{hlu} SET-C-020
9. PERFORMING ORGANIZATION NAME AND ADDRESS Systems Exploration, Inc. 3687 Voltaire St. San Diego, CA 92106 <i>S/C</i>	17	10. PROGRAM ELEMENT, PROJECT, TASK AREA & WORK UNIT NUMBERS 62721N; E21222 XF21222091 (B194)
11. CONTROLLING OFFICE NAME AND ADDRESS Naval Electronic Systems Command Code 3105 Washington, DC 20360	11	12. REPORT DATE 31 March 1978
14. MONITORING AGENCY NAME & ADDRESS (if different from Controlling Office) NAVAL OCEAN SYSTEMS CENTER San Diego, CA 92152 <i>(12) 103p.</i>		13. NUMBER OF PAGES
		15. SECURITY CLASS. (of this report) UNCLASSIFIED
		15a. DECLASSIFICATION/DOWNGRADING SCHEDULE
16. DISTRIBUTION STATEMENT (of this Report) Approved for public release; distribution unlimited.		
17. DISTRIBUTION STATEMENT (of the abstract entered in Block 20, if different from Report)		
18. SUPPLEMENTARY NOTES		
19. KEY WORDS (Continue on reverse side if necessary and identify by block number) High frequency FORTRAN Simulators Broadband Broadband Model Channels		
20. ABSTRACT (Continue on reverse side if necessary and identify by block number) A simulator has been developed that is capable of modeling the wideband HF channel. It is designed for carrier frequencies in the 2-32 MHz range and it can accommodate bandwidths up to 100 kHz and ground ranges up to 1000 km. It models the groundwave and ionosphere returns, but does not include additive noise or signal distortion produced in the transmitter or receiver. The inputs are the basic physical quantities that characterize the ionosphere (height, thickness, and maximum electron density of the E and F regions, sunspot number, time of day, etc) and those quantities that characterize the transmitter-receiver environment (carrier frequency, range, geographic location, antenna patterns, etc). Explicit values for channel parameters such as delay, attenuation, and doppler		

S/C 403972

1/B

UNCLASSIFIED

SECURITY CLASSIFICATION OF THIS PAGE(When Data Entered)

20. shift and spread are not required as these are calculated internally.

The simulator is divided into two parts. The first part is concerned with the mathematical model of the ionosphere and the computation of the channel parameters from the basic inputs. These channel parameters are used in the second part to determine the response for arbitrary inputs. A software version of the simulator has been implemented and tested, and a Fortran listing of the program is appended. The program runs in non-real time and requires a computer with a Fortran IV compiler and at least 28 K of core.

ACCESSION	
NTIS	Index Section <input checked="" type="checkbox"/>
DOC	Self Section <input type="checkbox"/>
UNCLASSIFIED	<input type="checkbox"/>
JUSTIFICATION	
BY	
DISTRIBUTION/AVAILABILITY CODES	
Dist.	AVAIL. and/or SPECIAL
A	

UNCLASSIFIED

SECURITY CLASSIFICATION OF THIS PAGE(When Data Entered)

OBJECTIVE

Develop a mathematical model for the wideband HF channel and the software implementation of this model. The model must be valid for carrier frequencies in the 2-32 MHz range, for bandwidths up to 100 kHz, and for ground ranges up to 1000 km.

RESULTS

A simplified model of the ionosphere is employed to determine the various skywave returns and the effect these returns have on the overall received signal. The groundwave is modeled as a delayed, attenuated version of the transmitted signal. Inputs to the simulator consist of those basic physical quantities that characterize the ionosphere and those that characterize the transmitter-receiver environment; values of delay, attenuation, doppler shift and spread, and dispersion are calculated internally for each component of the received signal. A FORTRAN version of the simulator has been written and tested for several typical channels.

RECOMMENDATIONS

Make further refinements in the mathematical model in order to expand the scope and accuracy of the simulator. Of particular value in this regard would be the inclusion of a deviative absorption term for the skywave returns and the inclusion of an attenuation term for propagation of the groundwave over a rough, lossy ocean surface.

Investigate the relationship between the simulator inputs and the actual observed returns as measured, for example, by an ionosonde. A knowledge of this relationship would provide further verification of the mathematical model as well as a set of inputs that correspond to known operating conditions.

Finally, in view of the meager data base available in the wideband case, any measurement program aimed at enlarging this data base would represent a significant contribution to the study and modeling of HF channels.

GLOSSARY

English Letter Symbols

a	Multiplicative constant used to generate random sequence $\{Y_n\}$
$a_j(n)$	Impulse response of filter used to generate approximate random gain $G_j(nT_0)$
A	Multiplicative constant for doppler shift
A_g	Gain of groundwave
A_j	RMS gain of j-th ionosphere path
$A(x)$	$= 2 G \tan \theta$
B	Multiplicative constant for doppler spread
B_r	Bearing of receiver as seen from transmitter in magnetic coordinates
BW	Two-sided bandwidth of transmitted signal
c	Velocity of light
$C_{G_j}(\tau)$	Correlation function of $G_j(t)$
$C_{G_j}^{\lambda}(\tau)$	Correlation function of $G_j^{\lambda}(t)$
$C_{U_j}(\tau)$	Correlation function of $U_j^{(1)}(t)$ and $U_j^{(2)}(t)$
D	Virtual path length
D_g	Delay of groundwave
$D_j^{(0)}$	$= f_c \cdot \tau_j^{(0)}$
$D_j^{(k)}$	$= \frac{1}{k!} [k\tau_j^{(k-1)} + f_c \tau_j^{(k)}], k = 1, 2, \dots$
f	Frequency
f_c	Carrier frequency

GLOSSARY (Continued)

f_r	Doppler reference frequency
f_{HD}	Gyrofrequency of D region
f_{HE}	Gyrofrequency of E region
f_{HF}	Gyrofrequency of F region
f_{pE}	General expression for penetration frequency of E region (ordinary or extraordinary wave)
f_{pF}	General expression for penetration frequency of F region (ordinary or extraordinary wave)
$f_{pE}^{(o)}$	Penetration frequency of E region - ordinary wave
$f_{pE}^{(x)}$	Penetration frequency of E region - extraordinary wave
$f_{pF}^{(o)}$	Penetration frequency of F region - ordinary wave
$f_{pF}^{(x)}$	Penetration frequency of F region - extraordinary wave
$G = G(f)$	Group height of signal path, oblique incidence
$G_j(t)$	Random gain of j-th path
$\tilde{G}_j(t)$	Approximation for random gain of j-th path
$G_R(\theta)$	Gain of receiving antenna
$G_T(\theta)$	Gain of transmitting antenna
$G_v = G_v(f)$	Group height of signal path, vertical incidence
h	Height above earth
h_D	Height of peak electron density of D region
h_E	Height of peak electron density of E region

GLOSSARY (Continued)

h_F	Height of peak electron density of F region
h_r	Height at which refractive index equals zero at vertical incidence
$h_j(t)$	Distortion impulse response of j-th path
$\hat{h}_j(t)$	Modified distortion impulse response: = $T_0 h_j(t)$
$2H_E$	Semithickness of E region electron density
$2H_F$	Semithickness of F region electron density
$H_j(f)$	Fourier transform of $h_j(t)$
I	Angle of inclination of earth's magnetic field
$I(x)$	Canonical expression representing general impulse response $\hat{h}_j(t)$
$I_p(x)$	Integrals used in series representation of $I(x)$
k	Sunspot number multiplier for non-deviative absorption loss
K	Multiplicative constant for non-deviative absorption loss
K_j	Constant used in the generation of $\hat{G}_j(nT_0)$
L_{abs}	Absorption loss
L_{ant}	Antenna pattern loss
L_d	Spreading loss
L_j	Total loss of j-th path
M	Length of pseudo random sequence
$N=N(h)$	Electron density
N_E	Maximum electron density of E region

GLOSSARY (Continued)

N_F	Maximum electron density of F region
N_g	Integer multiple of T_0 nearest the groundwave delay D_g
N_j	Integer multiple of T_0 nearest the signal delay D_j
$P_{G_j}(f)$	Power spectral density of $G_j(t)$
$P_{\tilde{G}_j}(f)$	Power spectral density of $\tilde{G}_j(t)$
$P_{U_j}(f)$	Power spectral density of $U_j^{(1)}(t)$ and $U_j^{(2)}(t)$
$r(t)$	Received, complex, baseband signal
R	Distance between transmitter and receiver
$s(t)$	Transmitted, complex, baseband signal
$\tilde{s}_j(t)$	Distorted, complex signal returned from ionosphere via j-th path
$\hat{s}_j(t)$	Distorted, complex signal returned from ionosphere via j-th path after removal of phase and delay components: $\tilde{s}_j(t) = \exp[-2\pi i D_j^{(0)}] \hat{s}_j(t - D_j^{(1)})$
S	Sunspot number
$S(f)$	Fourier transform of $s(t)$
t	Time
T_0	Sampling interval (one half the Nyquist interval of the transmitted signal)
u_1, u_2	Uniform [0,1] random variables
$U_j^{(1)}(t), U_j^{(2)}(t)$	Real, independent, zero mean identically-distributed, Gaussian process used to define $G_j(t)$
$W_j(1), W_j(2), W_j(3)$	Independent, complex, Gaussian random variables used in generation of $G_j(nT_0)$
x	$= \cos \theta$
$\{Y_n\}$	Sequence of pseudo random integers

GLOSSARY (Continued)

Greek Letter Symbols

α	Doppler shift exponent
β	Doppler spread exponent
γ	Exponent of solar zenith angle term in expression for nondeviative absorption
$\gamma_j(1), \gamma_j(2)$	Constants used in the generation of $\tilde{G}_j(nT_0)$
$\Delta^{(2)}$	General amplitude distortion coefficient
$\Delta^{(3)}$	General phase distortion coefficient
$\Delta_j^{(2)}$	Normalized amplitude distortion coefficient of j-th path
$\Delta_j^{(3)}$	Normalized phase distortion coefficient of j-th path
η	Normalized frequency variable = f/BW
θ	Ray angle of signal path measured from vertical
κ	$= (e^2/4\pi^2\epsilon_0 m) \approx 80.5$
λ	Geographic longitude
λ_0	Geographic longitude of north magnetic pole
$\lambda_j(1), \lambda_j(2)$	Constants used in the generation of $\tilde{G}_j(nT_0)$
μ	Refractive index
ν	General doppler shift
ν_j	Doppler shift of j-th path
ν_r	Reference doppler shift

GLOSSARY (Continued)

ξ	Complex Gaussian random variable
$\xi_j(n)$	Independent, identically-distributed Gaussian sequence
$\xi_j^{(1)}(n)$	Real part of $\xi_j(n)$
$\xi_j^{(2)}(n)$	Imaginary part of $\xi_j(n)$
ρ	Parameter used in fitting $C_{G_j}^{\lambda}(\tau)$ to $C_{G_j}(\tau)$
2σ	General doppler spread
$2\sigma_j$	Doppler spread of j-th path
$2\sigma_r$	Reference doppler spread
τ	General path delay
$\tau_j(f)$	Delay of j-th path as a function of frequency
$\tau_j^{(k)}$	k-th derivative of delay of j-th path evaluated at the carrier frequency f_c
ϕ	Geographic latitude
ϕ_0	Geographic latitude of north magnetic pole
Φ	Magnetic latitude
χ	Solar zenith angle
ψ_i	Angle between earth's magnetic field and wave incident upon ionosphere
ψ_r	Angle between earth's magnetic field and wave reflected from ionosphere

TABLE OF CONTENTS

<u>Section</u>	<u>Page</u>
I. INTRODUCTION.	1
II. THE HF CHANNEL	3
III. MATHEMATICAL MODEL OF THE IONOSPHERE.	10
A. Delay and Delay Derivatives	10
B. Attenuation	17
B.1 Absorption.	17
B.2 Antenna Gain	19
B.3 Spreading Loss	19
C. Doppler.	20
D. Computer Program.	22
IV. SIGNAL ANALYSIS.	29
A. Delay Distortion.	30
B. Random Gains	33
C. Computer Program.	34
V. CONCLUDING REMARKS.	36
VI. REFERENCES	38
Appendix A - Delay and Delay Derivatives.	A-1
Appendix B - Program for Calculating Channel Parameters	B-1
Appendix C - Computer Generation of Random Gains.	C-1
Appendix D - Signal Analysis Program	D-1

LIST OF FIGURES

<u>Figure</u>	<u>Page</u>
1 Block Diagram of Simulator.	9
2 Virtual and Actual Signal Paths	10
3 Nighttime Electron Density Profile	13
4 Daytime Electron Density Profile.	14
5 Computed Ionosphere Returns for One, Two and Three Hops.	28
6 Normalized Correlation Function for the Random Gains.	35

LIST OF TABLES

<u>Table</u>	<u>Page</u>
1 Default Values for Doppler Shift and Doppler Spread	22
2 Typical Output Listing for Computed Channel Parameters	23
3 Index Convention for Ionosphere Returns	25
4 Glossary of Terms used for Computed Channel Parameters	26
5 Typical Output Listing for Computed Channel Parameters (Includes only those Returns Having Attenuations within 40 dB of the Smallest Nonzero Attenuation)	27

I. INTRODUCTION

The use of channel simulators to study the performance of communication systems and to assist in their design has become increasingly popular in recent years. By employing a simulator, it is possible to reproduce given channel characteristics as desired and to compare different system designs in identical environments. Moreover, the cost of simulation is usually much less than the cost of "on the air" measurements and it is quite reliable. A variety of HF channel simulators have been proposed and studied in the past [1-4]*. Sailors and Hill [5] have written an excellent survey of the field and have made several recommendations for future work. Some of these recommendations are embodied in the present report.

In the following the development of a simulator for the wide-band HF channel is described. This simulator is designed for carrier frequencies in the 2-32 MHz range and it can accommodate bandwidths up to 100 kHz and ground ranges up to 1000 km. The simulator models the groundwave and all ionosphere returns (both single and multiple hops), but does not include additive noise or signal distortion produced in the transmitter or receiver. It takes into account all ionospheric phenomena that have a significant effect on wideband communications. Many of these phenomena, such as delay differences between the ordinary and extraordinary waves and signal distortion caused by variations of delay with frequency, have been neglected in the earlier simulators, resulting in severe bandwidth limitations. The inputs required are the basic parameters that characterize the physical ionosphere (height, thickness, and maximum electron density of the E and F regions, sunspot number, time of day, etc.) and those that characterize the transmitter and receiver (carrier frequency, range, geographic location, antenna patterns, etc.). Since these input parameters are the ones that are actually known in practice it is a simple matter to vary them and observe the effect they have on system performance. This

*References are listed in Section VI.

capability does not exist in the previous simulators which require as inputs not the basic quantities mentioned above but those channel parameters such as delay, attenuation, doppler shift and doppler spread derived from them.

In the course of developing the simulator a number of simplifications and approximations have been made to obtain tractable results. The most important of these assumptions concerns the electron density profile and the absorption mechanism. It is recognized that the ionosphere model used does not provide a detailed physical characterization of the ionosphere; however, it does provide an "order of magnitude" characterization suitable for communication purposes. The simulator is divided into two parts. The first part is concerned with the mathematical model of the ionosphere and the computation of the channel parameters from the basic inputs. The second part uses these parameters to determine the channel response for arbitrary inputs. Both parts of the simulator are described in detail in the following sections.

II. THE HF CHANNEL

The signal received via the HF channels considered in this report is the sum of the groundwave and the various ionosphere returns. Throughout we shall assume that the groundwave is an attenuated, delayed version of the transmitted signal but is otherwise undistorted. The ionosphere returns also suffer attenuation and delay but in addition are subject to fading and distortion. There is also time dispersion (multipath) produced by the different delays associated with each ionosphere return. The purpose of this section is to present some definitions that are used in the sequel and to introduce the mathematical model for the HF channel.

The complex transmitted baseband signal will be denoted by $s(t)$ and its Fourier transform by $S(f)$. Thus

$$s(t) = \int_{-\infty}^{\infty} S(f) \exp [2\pi i f t] df. \quad (1)$$

Distorted versions of this signal will be returned from the ionosphere for both the E region and the F region (low ray and high ray). There will be a set of these returns for the ordinary and extraordinary magnetoionic components and for as many multiple-hop paths as are present. Although many returns are possible, all but a few of these experience a large attenuation and the number of effective returns is usually small. In the following we will denote the number of effective ionosphere returns by N . This number is determined by excluding all returns that suffer an attenuation greater than some predetermined value.

Distortion of signals reflected from the ionosphere has been studied by several authors, who have attempted to characterize the impulse response for a simplified model of the ionosphere [6-10]. Unfortunately, these results have been derived using ionosphere

models that are too idealized for our purposes¹ and the impulse responses obtained are too complicated for easy implementation². In order to obtain tractable expressions for the distortion we shall assume that it is caused primarily by the fact that the delay is a function of frequency and is not constant across the signal bandwidth. This characterization of the distortion mechanism allows us to make a number of approximations which result in relatively simple expressions for the distorted signal. For obvious reasons we shall refer to this particular distortion as delay distortion.

Let f_c denote the carrier frequency and let $\tau_j(f)$ denote the delay of the j -th return as a function of frequency. It follows from (1) that the distorted baseband signal returned from the ionosphere is given by

$$\tilde{s}_j(t) = \int_{-\infty}^{\infty} S(f) \exp [-2\pi i(f_c+f) \cdot \tau_j(f_c+f)] \cdot \exp [2\pi i f t] df. \quad (2)$$

$j = 1, \dots, N$

We will characterize this distortion by the coefficients in the power series expansion of the delay about the carrier frequency. This series appears as

$$\tau_j(f_c+f) = \sum_{k=0}^{\infty} \frac{f^k}{k!} \tau_j^{(k)}, \quad j=1, \dots, N \quad (3)$$

¹They allow for reflection only from a single ionospheric region and consider such simple electron density profiles as a constant and a linear function of height.

²In one case the impulse response is given as the solution of an integral equation.

with

$$\tau_j^{(k)} = \frac{d^k}{df^k} \tau_j(f_c + f) \Big|_{f=0} \quad (4)$$

Substituting this series into the exponential delay term in (2) we obtain

$$\exp[-2\pi i (f_c + f) \cdot \tau_j(f_c + f)] = \exp \left[-2\pi i \sum_{k=0}^{\infty} f^k D_j^{(k)} \right] \quad (5)$$

$j=1, \dots, N$

where we have defined

$$D_j^{(0)} = f_c \tau_j^{(0)} \quad j=1, \dots, N \quad (6)$$

and

$$D_j^{(k)} = \frac{1}{k!} \left[k \tau_j^{(k-1)} + f_c \tau_j^{(k)} \right] \quad \begin{array}{l} k=1, 2, \dots \\ j=1, \dots, N. \end{array} \quad (7)$$

Thus, for $\tilde{s}_j(t)$ we have

$$\tilde{s}_j(t) = \exp[-2\pi i D_j^{(0)}] \int_{-\infty}^{\infty} s(f) \exp \left[-2\pi i \sum_{k=2}^{\infty} f^k D_j^{(k)} \right] \cdot \exp \left[2\pi i f (t - D_j^{(1)}) \right] df. \quad (8)$$

$j=1, \dots, N$

For computational reasons it is convenient to separate the phase and delay terms from the actual distortion of the signal. To this end we define a function $\hat{s}_j(t)$ as follows

$$\tilde{s}_j(t) = \exp[-2\pi i D_j^{(0)}] \hat{s}_j(t - D_j^{(1)}) \quad (9)$$

$j=1, \dots, N$

where

$$\hat{s}_j(t) = \int_{-\infty}^{\infty} s(f) H_j(f) \exp[2\pi i f t] df, \quad j=1, \dots, N \quad (10)$$

with

$$H_j(f) = \exp\left[-2\pi i \sum_{k=2}^{\infty} f^k D_j^{(k)}\right], \quad j=1, \dots, N. \quad (11)$$

In practice it is convenient to determine $\hat{s}_j(t)$ by performing a time domain convolution rather than by evaluating the Fourier transform (10). If the impulse response determined by $H_j(f)$ is denoted by $h_j(t)$, we have

$$h_j(t) = \int_{-\infty}^{\infty} H_j(f) \exp[2\pi i f t] df, \quad j=1, \dots, N., \quad (12)$$

and the desired convolution appears as

$$\hat{s}_j(t) = \int_{-\infty}^{\infty} s(t-u) h_j(u) du, \quad j=1, \dots, N. \quad (13)$$

A discussion of the approximations used in the numerical evaluation of $h_j(t)$ and $\hat{s}_j(t)$ is presented in Section IV.

In addition to the above distortion, the ionosphere returns are subject to attenuation and random fading. These two phenomena are included by multiplying the delayed, distorted signal by a random gain, which we denote by $G_j(t)$. We will assume that $G_j(t)$ is a complex, zero-mean, Gaussian process with identically-distributed real and imaginary parts. This is the Rayleigh fading model [11]. While the assumption of Rician fading [12] would provide somewhat more flexibility than the Rayleigh assumption, the available evidence [12-14] indicates that the Rayleigh model is adequate for our purposes. The random gains associated with different returns are assumed to be independent.

Let $U_j^{(1)}(t)$ and $U_j^{(2)}(t)$ denote two real, independent zero mean, identically-distributed, stationary Gaussian processes with correlation function

$$C_{U_j}(\tau) = E U_j^{(1)}(t+\tau)U_j^{(1)}(t) = E U_j^{(2)}(t+\tau)U_j^{(2)}(t). \quad (14)$$

$j=1, \dots, N.$

The corresponding power spectral density is given by

$$P_{U_j}(f) = \int_{-\infty}^{\infty} C_{U_j}(\tau) \exp[-2\pi i f \tau] d\tau, j=1, \dots, N. \quad (15)$$

We define the random gain in terms of $U_j^{(1)}(t)$ and $U_j^{(2)}(t)$ as follows

$$G_j(t) = [U_j^{(1)}(t) + i U_j^{(2)}(t)] \cdot \exp[2\pi i v_j t] \quad (16)$$

$j=1, \dots, N.$

where v_j is the doppler shift for the j -th ionosphere return. The correlation and power spectral density of $G_j(t)$ are easily determined using the assumed properties of $U_j^{(1)}$ and $U_j^{(2)}$. Thus

$$C_{G_j}(\tau) = E G_j(t+\tau)G_j^*(t) = 2C_{U_j}(\tau) \cdot \exp[2\pi i v_j \tau] \quad (17)$$

$j=1, \dots, N.$

and

$$P_{G_j}(f) = 2P_{U_j}(f-v_j), \quad j=1, \dots, N. \quad (18)$$

Following Watterson [1] we assume that the power spectral density $P_{G_j}(f)$ has a Gaussian shape. While there is no conclusive experimental evidence for this assumption, it is a convenient model for spectra that are unimodal and that decrease rapidly. Specifically we let

$$C_{G_j}(\tau) = A_j^2 \exp[-2\pi^2 \sigma_j^2 \tau^2 + 2\pi i v_j \tau] \quad . \quad (19)$$

$j=1, \dots, N$

Here A_j is the rms gain ($0 \leq A_j \leq 1$) of the j -th return and $2\sigma_j$ is the doppler spread of the return. The power spectral density associated with this correlation function is

$$P_{G_j}(f) = \frac{A_j^2}{\sqrt{2\pi} \sigma_j} \exp \left[-\frac{(f-v_j)^2}{2\sigma_j^2} \right] \quad , \quad j=1, \dots, N. \quad (20)$$

Finally, we must add the groundwave to the ionosphere returns. The groundwave is assumed to experience only delay and to have a non-random gain. If A_g denotes the gain ($0 \leq A_g \leq 1$) and D_g denotes the delay, the contribution to the received signal from the groundwave is given by $A_g s(t-D_g)$. The gain is a complicated function of range, sea state and frequency. Graphs of this functional relationship are given in [15].

Summarizing the above, the complex, baseband received signal can be expressed as

$$r(t) = A_g s(t-D_g) + \sum_{j=1}^N \exp[-2\pi i D_j^{(0)}] G_j(t) \hat{s}_j(t-D_j^{(1)}) \quad . \quad (21)$$

A block diagram illustrating (21) is presented in Figure 1.

In the following sections, the quantities needed in the evaluation of $r(t)$ are derived and the techniques employed in its numerical evaluation are described.

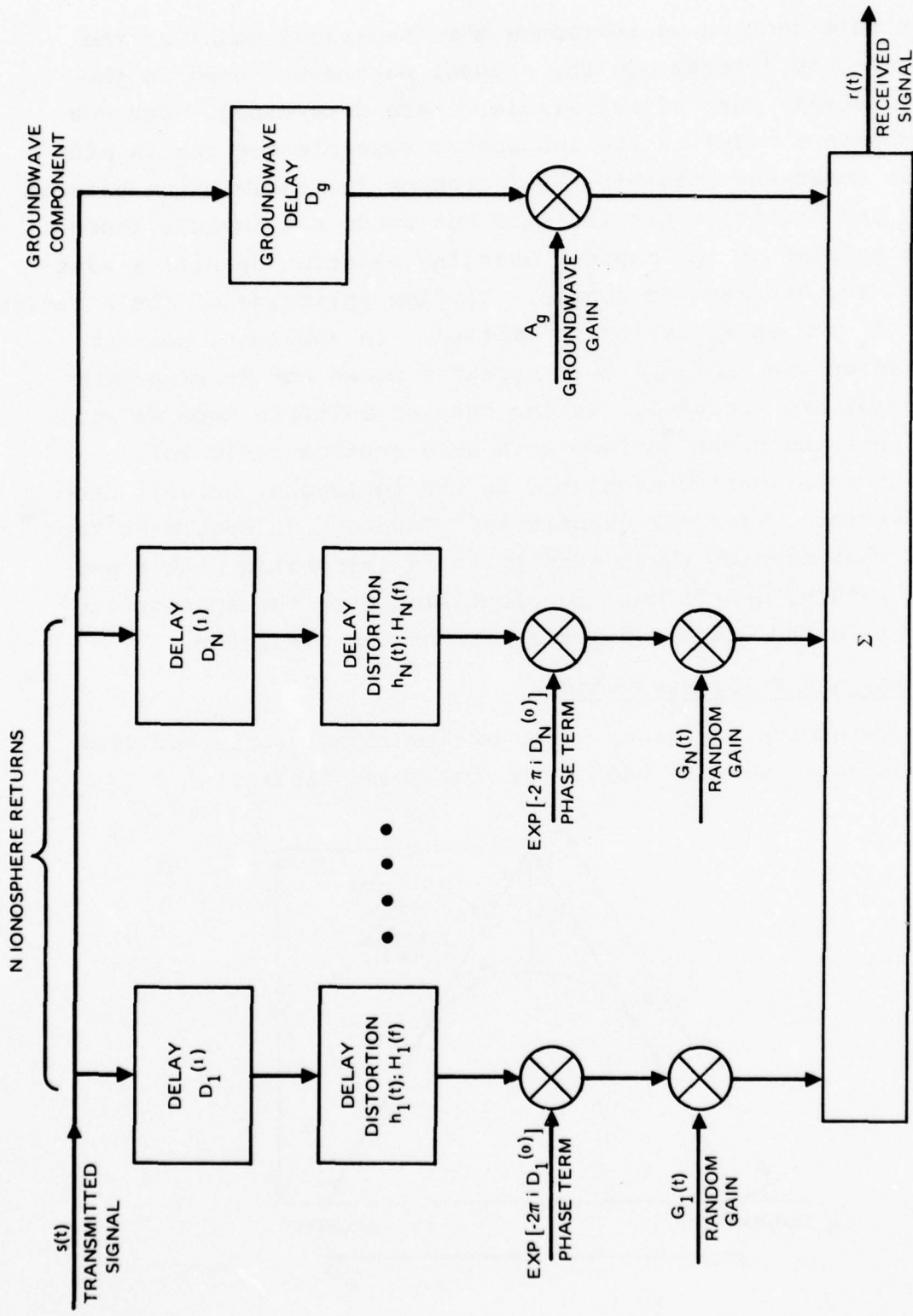


Figure 1. Block Diagram of Simulator

III. MATHEMATICAL MODEL OF THE IONOSPHERE

In this section we introduce a mathematical model of the ionosphere and discuss how the channel parameters used in the signal analysis part of the simulator are determined. Our goal is to obtain a model of the ionosphere suitable for use in mid-latitude ocean environments. Differences in transmission between daytime and nighttime are included but we do not include those effects related to the rapidly changing electron densities that occur during sunrise and sunset. Daytime splitting of the F region into an F_1 and an F_2 region is omitted. In addition, neither transmission via sporadic E or spread F modes nor M- or N-type reflections are included. In the case of multiple hops we will assume that the ocean surface acts as a perfect reflector.

As a notational convenience in the following, we will drop the subscript j from all quantities. However, it should be kept in mind that each of these quantities is associated with a particular return, and it must be identified with the appropriate subscript in the signal analysis part of the simulator.

A. Delay and Delay Derivatives

To determine the group delay of the signal reflected from the ionosphere, we make use of the following figure.

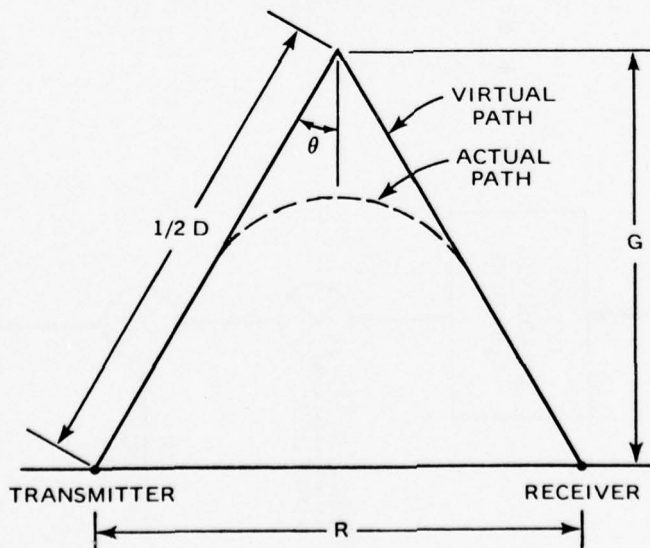


Figure 2. Virtual and Actual Signal Paths

Here the dashed line is the actual ionospheric path of the signal between the transmitter and the receiver and the solid line is the virtual path. The ground range between transmitter and receiver is denoted by R , the virtual path length by D , the ray angle measured from the vertical by θ and the group height by G . Assuming a flat earth and ionosphere, we have by simple geometry

$$D = \frac{R}{\sin \theta} = \frac{R}{(1-x^2)^{\frac{1}{2}}} \quad (22)$$

where we have defined $x = \cos \theta$. If c denotes the velocity of light, the signal delay is given by the virtual path length divided by c

$$\tau = \frac{R}{c(1-x^2)^{\frac{1}{2}}} \quad (23)$$

It remains to determine the ray angle θ .

For vertical incidence ($\theta=0$), the group height is given by the integral [16]

$$G_V = G_V(f) = \int_0^{h_r} \frac{dh}{\mu} \quad (24)$$

where μ is the refractive index and h_r is the height at which $\mu=0$. In the absence of both collisions and the earth's magnetic field, the refractive index is given by [16]

$$\mu^2 = \left(1 - \kappa \frac{N}{f^2}\right) \quad (25)$$

where $N = N(h)$ is the electron density in m^{-3} , f is the frequency in Hz and $\kappa = (e^2/4\pi^2\epsilon_0 m) \approx 80.5$. The group height for oblique incidence is the same as for vertical incidence but we must replace f by $f \cos \theta$ [16]. That is $G = G(f) = G_V(f \cos \theta)$. Once the group height has been determined, we appeal to Figure 2 to obtain the relationship

$$R = 2 G \tan \theta = 2 G \left(\frac{1-x^2}{x^2}\right)^{\frac{1}{2}} \quad (26)$$

Defining

$$A(x) = 2 G \left(\frac{1-x^2}{x} \right)^{1/2} \quad (27)$$

we see that, for a specified range R , we must solve the transcendental equation

$$R = A(x) \quad (28)$$

for x and then substitute this into (23) to obtain the delay.

We seek an approximation to the electron density for which the group height, G , can be expressed in a simple closed form. Our main concern here is with reflections from the E and F regions. At nighttime we assume that the electron density profile can be represented by two distinct parabolas as shown in Figure 3. Let N_E be the peak electron density of the E region in m^{-3} , let h_E be the height of the peak electron density of the E region in km, and let $2H_E$ be the semithickness of the E region in km; similar definitions are made for the F region. Then the nighttime electron density is given by

$$N(h) = \begin{cases} 0 & h < h_E - 2H_E \\ N_E \left[1 - \left(\frac{h-h_E}{2H_E} \right)^2 \right] & h_E - 2H_E < h < h_E + 2H_E \\ 0, \left(\frac{h-h_F}{2H_F} \right)^2 & h_E + 2H_E < h < h_F - 2H_F \\ N_F \left[1 - \left(\frac{h-h_F}{2H_F} \right)^2 \right] & h_F - 2H_F < h < h_F + 2H_F \\ 0 & h_F + 2H_F < h \end{cases} \quad (29)$$

In the daytime the electron density profile is also assumed to be parabolic but allowance is made for ionization between the E and F regions. The electron density between the two regions is assumed to be constant and equal to the peak value of the E region. This is illustrated in Figure 4. Using the same definitions as before, the daytime electron density is given by

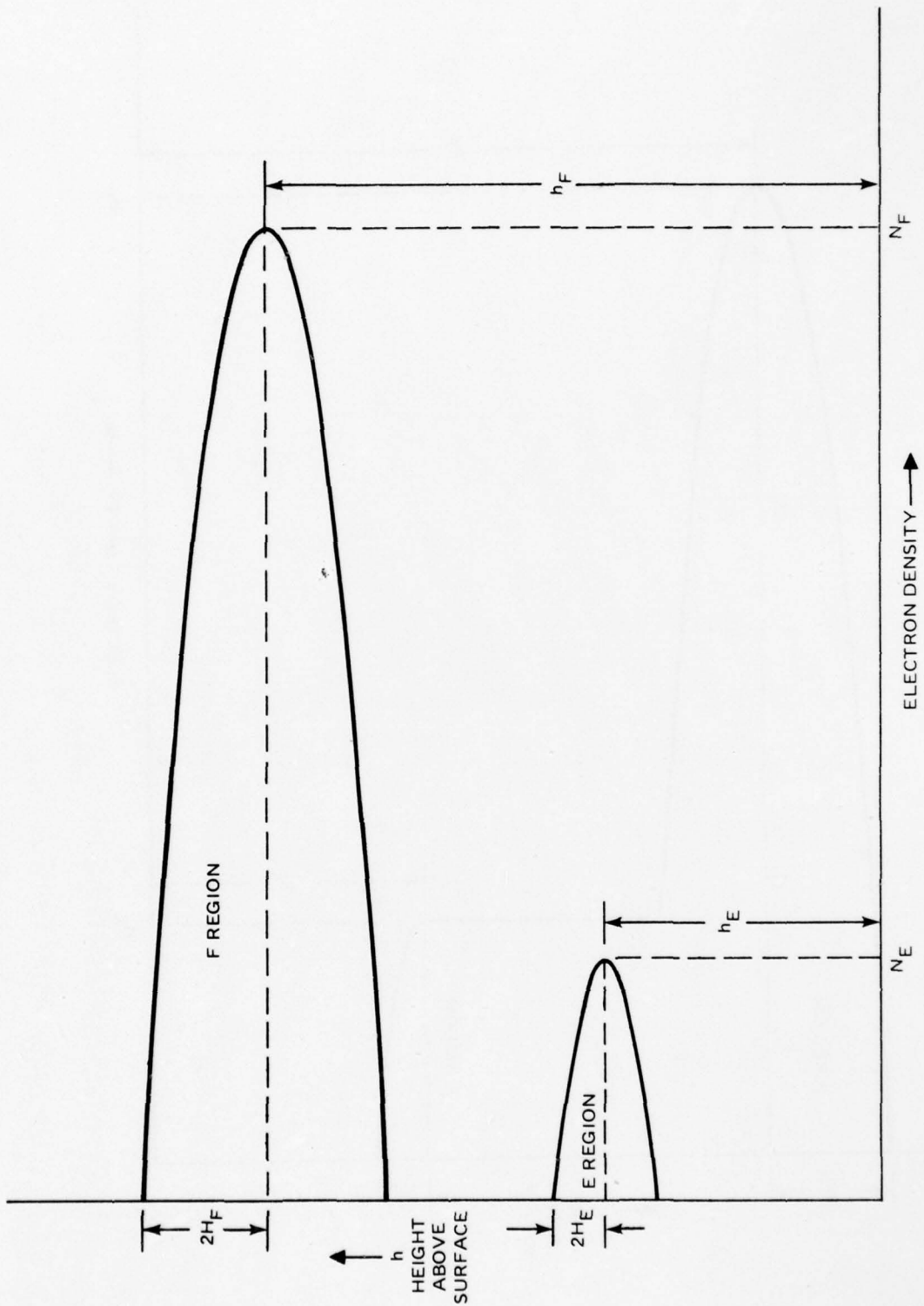


Figure 3. Nighttime Electron Density Profile

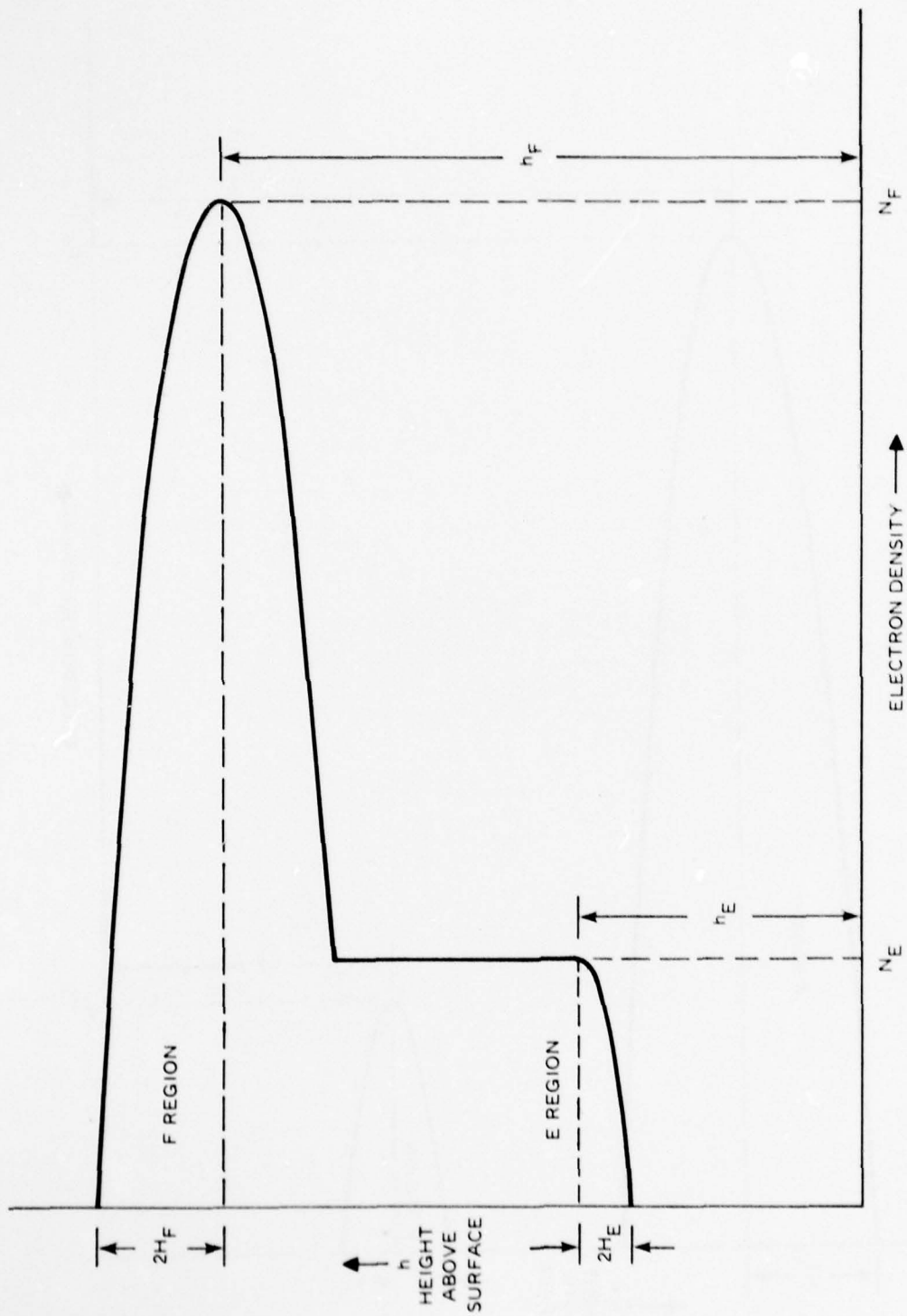


Figure 4. Daytime Electron Density Profile

$$N(h) = \begin{cases} 0, & h < h_E - 2H_E \\ N_E \left[1 - \left(\frac{h - h_E}{2h_E} \right)^2 \right], & h - 2H_E < h < h_E \\ N_E, & h_E < h < h_F + 2H_F \left(1 - \frac{N_E}{N_F} \right)^{\frac{1}{2}} \\ N_F \left[1 - \left(\frac{h - h_F}{2h_F} \right)^2 \right], & h_F + 2H_F \left(1 - \frac{N_E}{N_F} \right)^{\frac{1}{2}} < h < h_F + 2H_F \\ 0, & h_F + 2H_F < h. \end{cases} \quad (30)$$

Note that the constants appearing in (24) and (30) will be different owing to the different heights and ionization densities for nighttime and daytime conditions.

A quantity of interest in the present analysis is the penetration frequency of each region. This is defined as the plasma frequency at the peak electron density [16]. We have for the E and F regions

$$f_{pE}^2 = \kappa N_E \quad (31a)$$

$$f_{pF}^2 = \kappa N_F \quad (31b)$$

where $\kappa = (e / 4\pi^2 \epsilon_0 m) \approx 80.5$ and the two penetration frequencies are in Hz. The physical interpretation of f_{pE} and f_{pF} is that they represent the maximum frequencies at which signals will be reflected from the respective regions at vertical incidence.

Returning to the determination of the group height, G , it is a relatively simple matter to evaluate the integral (24) for either of the above electron densities [17]. The details of this evaluation are presented in Appendix A.

In the foregoing the effect of the earth's magnetic field has been neglected, but we take this to be an adequate approximation for the ordinary wave. For the extraordinary wave, however, the penetration frequencies are shifted relative to those for the ordinary wave, and it is essential to take this into account.

Denoting the penetration frequencies of the ordinary and extraordinary waves by the superscripts "o" and "x" we have [16]

$$f_{pE}^{(x)} = \frac{1}{2} f_{HE} + \left[f_{HE}^2 + 4 (f_{pE}^{(o)})^2 \right]^{1/2} \quad (32a)$$

$$f_{pF}^{(x)} = \frac{1}{2} f_{HF} + \left[f_{HF}^2 + 4 (f_{pF}^{(o)})^2 \right]^{1/2} \quad (32b)$$

Here $f_{pE}^{(o)}$ and $f_{pF}^{(o)}$ are defined by (31), and f_{HE} and f_{HF} are the gyrofrequencies associated with the earth's magnetic field at the levels of maximum ionization density in the E and F regions. For the gyrofrequencies in mHz we will use the approximate expressions [16]

$$f_{HE} = 0.87 \left(\frac{6370}{6370 + h_E} \right)^3 (1 + 3 \sin^2 \phi)^{1/2} \quad (33a)$$

$$f_{HF} = 0.87 \left(\frac{6370}{6370 + h_F} \right)^3 (1 + 3 \sin^2 \phi)^{1/2} \quad (33b)$$

where ϕ is the latitude expressed in magnetic coordinates. If ϕ and λ are respectively the geographic latitude and longitude, and ϕ_0 and λ_0 represent the latitude and longitude of the north magnetic pole ($\phi_0 \approx 78.3^\circ N$, $\lambda_0 \approx 69^\circ W$), then [16]

$$\sin \phi = \sin \phi \sin \phi_0 + \cos \phi \cos \phi_0 \cos (\lambda - \lambda_0) \quad (34)$$

We assume that, to calculate delays for the extraordinary wave, we may use the expressions in Appendix A but with $f_{pE}^{(x)}$ and $f_{pF}^{(x)}$ substituted for the ordinary wave penetration frequencies. Otherwise the calculations of delay are assumed to take the same form as those for the ordinary wave.

To characterize delay distortion we need the derivatives of the delay evaluated at the carrier frequency. Actually, only the first three derivatives are required for the approximation discussed in Section IV. The determination of these three derivatives is straightforward although the resulting expressions are quite complicated. They are listed in Appendix A.

For multiple hop transmissions we assume that the ionosphere parameters are identical for each hop. In the two-hop case the foregoing analysis is applied with the original range multiplied by 1/2. The angle is then correct as calculated but the path length, delay and delay derivatives must be multiplied by 2. Higher numbers of hops are treated in a similar manner using appropriate multipliers.

B. Attenuation

Three main sources of attenuation are included in the present model. They are: (1) nondeviative absorption, (2) antenna gain, and (3) spreading ($1/r^2$ loss). Other factors such as focusing and polarization mismatch will also affect the received signal strength, but these are assumed to be of secondary importance and they have accordingly been omitted.

B.1 Absorption

Absorption is assumed to take place only in the D region of the ionosphere and only in the daytime. The absorption is assumed to be nondeviative, i.e., it takes place in a region where the refractive index is near unity. The attenuation will be characterized by the expression [16]

$$L_{\text{abs}} = K \sec \theta \cdot (1+kS) \cdot (\cos \chi)^\gamma \quad (35)$$

$$\cdot \left\{ \frac{1}{(f \pm f_{\text{HD}} |\cos \psi_i|)^2} + \frac{1}{(f \pm f_{\text{HD}} |\cos \psi_r|)^2} \right\}$$

Here L_{abs} is the attenuation due to absorption in decibels per hop, θ is the ray angle measured from the vertical, S is the sunspot number, χ is the solar zenith angle, f is the frequency in MHz, f_{HD} is the gyrofrequency at the D region level in MHz and ψ_i [resp., ψ_r] is the angle between the earth's magnetic field and the incident [resp., reflected] wave. The plus sign is used for the ordinary wave and the minus sign is used for the extraordinary wave.

The relative importance of the sunspot number and solar zenith angle depends upon the constants K , k and γ ; following Davies [16, p. 235] we will set $K = 215$, $k = 0.0035$ and $\gamma = 0.75$. The gyrofrequency, f_{HD} , is given by [16]

$$f_{\text{HD}} = 0.87 \left(\frac{6370}{6370+h_D} \right)^3 (1+3 \sin^2 \phi)^{\frac{1}{2}} \quad (36)$$

where h_D is the height of the D region in km and ϕ is the latitude in magnetic coordinates. In this expression we will take h_D to be 70 km and use (34) to determine $\sin \phi$. The angles ψ_i and ψ_r are determined from the relationships

$$\cos \psi_i = \sin \theta \cos B_r \cos I + \cos \theta \sin I \quad (37a)$$

$$\cos \psi_r = \sin \theta \cos B_r \cos I - \cos \theta \sin I \quad (37b)$$

where B_r is the bearing of the receiver as seen from the transmitter in magnetic coordinates and I , the angle of inclination of the earth's magnetic field, is given by

$$\tan I = -2 \tan \phi. \quad (38)$$

For multiple-hop paths, the expression (35) must be multiplied by the number of hops.

B.2 Antenna Gain

No attempt has been made in this model to provide a variety of antenna patterns. While any desired antenna gain can be easily included in the program, we shall use the gain of a short vertical dipole for both transmitter and receiver. If G_T and G_R denote the transmitter and receiver power gains relative to isotropic antennas we have

$$G_T(\theta) = G_R(\theta) = \frac{3}{2} \sin^2 \theta. \quad (39)$$

Thus for the overall attenuation in decibels we have

$$L_{\text{ant}} = -10 \log_{10} G_T(\theta) - 10 \log_{10} G_R(\theta) = -20 \log_{10} \left[\frac{3}{2} \sin^2 \theta \right]. \quad (40)$$

B.3 Spreading Loss

The decrease in signal strength attributable to the length of the transmission path is given by

$$L_d = 20 \log_{10} \left(\frac{4\pi Df}{0.3} \right) \quad (41)$$

where L_d is the path loss in decibels, D is the total path length in km, taking into account any multiple hops, and f is the frequency in MHz.

The total attenuation for a particular ionosphere return is obtained by adding (35), (40) and (41), after making any necessary adjustments for multiple hops. Denoting the total attenuation for the j -th return by L_j we have

$$L_j = L_{\text{abs}} \times (\text{No. of Hops}) + L_{\text{ant}} + L_d. \quad (42)$$

The rms gain A_j is thus given by

$$A_j = 10^{-(L_j/20)} . \quad (43)$$

C. Doppler

The remaining quantities needed to characterize the random gains, $G_j(t)$, are the doppler shifts and the doppler spreads. In this report we are not concerned with the relatively large doppler values that occur during sunrise and sunset, but with the smaller values that are typical of the ionosphere for the majority of a typical twenty-four hour period. What is desired is the shift and spread associated with each of the propagation modes. Unfortunately, measurements that have been made concerning doppler values usually have not been concerned with the shift and spread of the individual propagation modes; instead they have recorded composite doppler values involving many modes [18]. Moreover, most theoretical studies have not been concerned with communication system performance and are of marginal value for present purposes [19-22].

What is required for our model is an expression relating the doppler shifts and spreads to frequency for each ionosphere return. This expression will depend on the electron density profile and its time rate of change as well as on various other ionosphere parameters [23]. We assume that the doppler values can be characterized adequately by the following power laws

$$\nu = A f^\alpha \quad (44)$$

and

$$\sigma = B f^\beta \quad (45)$$

where ν and 2σ are the doppler shift and doppler spread; f is the frequency in MHz; and A , B , α , and β are constants that characterize the region from which the wave is reflected and the magnetoionic

component involved. In general we need an expression of the above type for the low and high ray returns from each region and for each magnetoionic component.

It is convenient to express the constants A and B appearing in (44) and (45) in terms of a reference value measured at a known frequency. Thus the above expressions can be rewritten as

$$\nu = \nu_r (f/f_r)^\alpha \quad (46)$$

$$\sigma = \sigma_r (f/f_r)^\beta \quad (47)$$

where ν_r and $2\sigma_r$ are the doppler shift and spread measured at the reference frequency f_r . For multiple hops we assume that the doppler effects combine incoherently so that

$$\nu = (\text{No. of Hops}) \cdot \nu_r \cdot (f/f_r)^\alpha \quad (48)$$

and

$$\sigma = (\text{No. of Hops})^{1/2} \cdot \sigma_r \cdot (f/f_r)^\beta \quad (49)$$

Given the appropriate reference values and exponents, the above expressions provide the doppler shift and spread for each ionosphere return. However, since the reference values and exponents usually are not known, we must make some assumptions to obtain "default" values for use in the absence of more accurate data. It will be assumed that the doppler shift and spread are the same for the high ray and low ray and for both magnetoionic components of the E and F region returns. The following table gives the "default" reference values and exponents to be used for the E and F regions. These values are based upon measurements made by Watterson, et. al. [1].

Region	ν_r (Hz)	$2\sigma_r$ (Hz)	f_r (mHz)	α	β
E	0.01	0.02	9.30	1.0	1.0
F	0.01	0.15	9.30	1.0	1.0

Table 1. Default Values for Doppler Shift and Doppler Spread

D. Computer Program

The Fortran program used to calculate the foregoing channel parameters is presented in Appendix B. The basic output of this program is a listing of the input parameters and a tabular presentation of the computed channel parameters. A typical output is shown in Table 2. The indexing convention used for the returns is presented in Table 3 and a glossary of the terms used in the output is presented in Table 4.

A modified version of this output can be produced in which all returns whose attenuation exceeds some threshold value above the minimum attenuation are omitted. Those modes for which there is no return are likewise omitted. Using this modified output one can identify those returns that are of primary interest for communication purposes. An example is shown in Table 5 using the same inputs that produced Table 2 and an attenuation threshold of 40 dB.

A synthetic ionogram also has been produced using the program. The resulting curves are presented in Figure 5 and include returns for one, two and three hops together with the corresponding attenuations.

Table 3. Index Convention for Ionosphere Returns

Index	Number of Hops	Region	Ordinary or Extraordinary	Low Ray or High Ray
1	1	E	O	LOW
2	1	E	O	HIGH
3	1	F	O	LOW
4	1	F	O	HIGH
5	1	E	X	LOW
6	1	E	X	HIGH
7	1	F	X	LOW
8	1	F	X	HIGH
9	2	E	O	LOW
10	2	E	O	HIGH
11	2	F	O	LOW
.
.
.
44	6	F	O	HIGH
45	6	E	X	LOW
46	6	E	X	HIGH
47	6	F	X	LOW
48	6	F	X	HIGH

Table 4. Glossary of Terms Used
for Computed Channel Parameters

Mode	Identifies particular ionosphere return (e.g., 2FO LOW is the two-hop, F region, ordinary wave, low ray return)
Solution Indicator	This equals 1 if there is a return for the particular mode and equals 0 if there is no return
Ray Angle	θ_j
Total Path Length	D_j
Carrier Delay	$\tau(f_c)$
Carrier Phase	The fractional part of $D_j^{(0)}$
Signal Delay	$D_j^{(1)}$
Amplitude Distortion	$D_j^{(2)}$
Phase Distortion	$D_j^{(3)}$
Attenuation	L_j
Doppler Shift	v_j
Doppler Spread	$2\sigma_j$

Table 5. Typical Output Listing For Computed Channel Parameters
 (Includes Only Those Returns Having Attenuations Within 40dB Of The Smallest Nonzero Attenuation)

SUMMARY OF TRANSMISSION PARAMETERS

SIGNAL PARAMETERS

CARRIER FREQ. = 5.000 MHZ. BANDWIDTH = 100.00 MHZ.

TRANSMITTER/RECEIVER PARAMETERS

LOCATION OF TRANSMITTER: LONGITUDE = 150.00 DEGREES (+ FOR WEST, - FOR EAST)
 LATITUDE = 30.00 DEGREES (+ FOR NORTH, - FOR SOUTH)

DISTANCE BETWEEN TRANSMITTER AND RECEIVER = 500.00 KM.
 DIRECTION FROM TRANSMITTER TO RECEIVER = 0.00 DEGREES (MEASURED FROM TRUE NORTH)

TRANSMITTER ANTENNA PATTERN = (3/2)*(SIN(THETA)**2)
 RECEIVER ANTENNA PATTERN = (3/2)*(SIN(THETA)**2)
 SEA STATE = 1

IONOSPHERE PARAMETERS

SUNSPOT NUMBER = 100.00
 SOLAR ZENITH ANGLE = 45.00 DEGREES
 DAYTIME ELECTRON DENSITY PROFILE

E REGION HEIGHT OF MAX. ELECTRON DENSITY = 110.00 KM.
 PERMITTIVITY OF PARABOLA = 20.00 KM.
 PENETRATION FREQUENCY, ORDINARY WAVE = 2.000 MHZ.
 PENETRATION FREQUENCY, EXTRAORDINARY WAVE = 2.030 MHZ.

F REGION HEIGHT OF MAX. ELECTRON DENSITY = 250.00 KM.
 PERMITTIVITY OF PARABOLA = 50.00 KM.
 PENETRATION FREQUENCY, ORDINARY WAVE = 8.000 MHZ.
 PENETRATION FREQUENCY, EXTRAORDINARY WAVE = 8.537 MHZ.

NONDEVIATIVE ABSORPTION CONSTANTS
 MULTIPLICATIVE CONSTANT = 215.00, SUNSPOT NUMBER MULTIPLIER = 0.003500, SOLAR ZENITH ANGLE EXPONENT = 0.750

DOPPLER REFERENCE VALUES
 E REGION SHIFT = 0.0100 HZ, SHIFT EXP. = 1.0003 SPREAD = 0.0200 HZ, SPREAD EXP. = 1.0003 RLF, FREQ. = 9.300 MHZ.
 F REGION SHIFT = 0.0100 HZ, SHIFT EXP. = 1.0003 SPREAD = 0.1200 HZ, SPREAD EXP. = 1.0003 REF, FREQ. = 9.300 MHZ.

COMPUTED CHANNEL PARAMETERS

GROUNDWAVE DELAY = 1.667E-03 SEC. ATTENUATION = 1.200E+02 DB.
 IONOSPHERE RETURNS:

MODE	SOLUTION INDICATOR (0=NO SOLN)	HAY ANGLE (DEGREES)	PATH LENGTH (KM)	CARRIER DELAY (SEC)	CARRIER PHASE (CYCLES)	SIGNAL DELAY (SEC)	AMPLITUDE DISTURBANCE (SEC/MHZ)	PHASE DISTURBANCE (SEC/MHZ**2)	ATTENUATION (DB)	DUPPLER SHIFT (MHZ)	DOPPLER SPREAD (MHZ)
1FD LOW	NA	86.91	688.68	2.222E-03	8.094E-01	2.096E-03	5.760E-05	1.348E-05	1.265E+02	5.376E-03	8.065E-02
1FX LOW	NA	67.53	581.07	1.804E-03	7.755E-01	1.933E-03	1.098E-04	9.042E-05	1.619E+02	5.376E-03	1.075E-02
1FX HIGH	NA	58.18	587.19	1.957E-03	8.458E-01	1.616E-03	7.306E-05	-1.595E-04	1.805E+02	5.376E-03	1.075E-02
1FX LOW	NA	44.11	718.30	2.339E-03	6.671E-01	1.824E-03	1.444E-04	2.562E-05	1.801E+02	5.376E-03	8.065E-02
2FD LOW	NA	28.55	1046.08	3.447E-03	6.699E-01	3.583E-03	1.991E-04	4.136E-05	1.471E+02	1.075E-02	1.140E-01

ALL IONOSPHERIC RETURNS WHOSE ATTENUATION IS GREATER THAN 40.00 DB ABOVE THE MINIMUM ATTENUATION ARE IGNORED

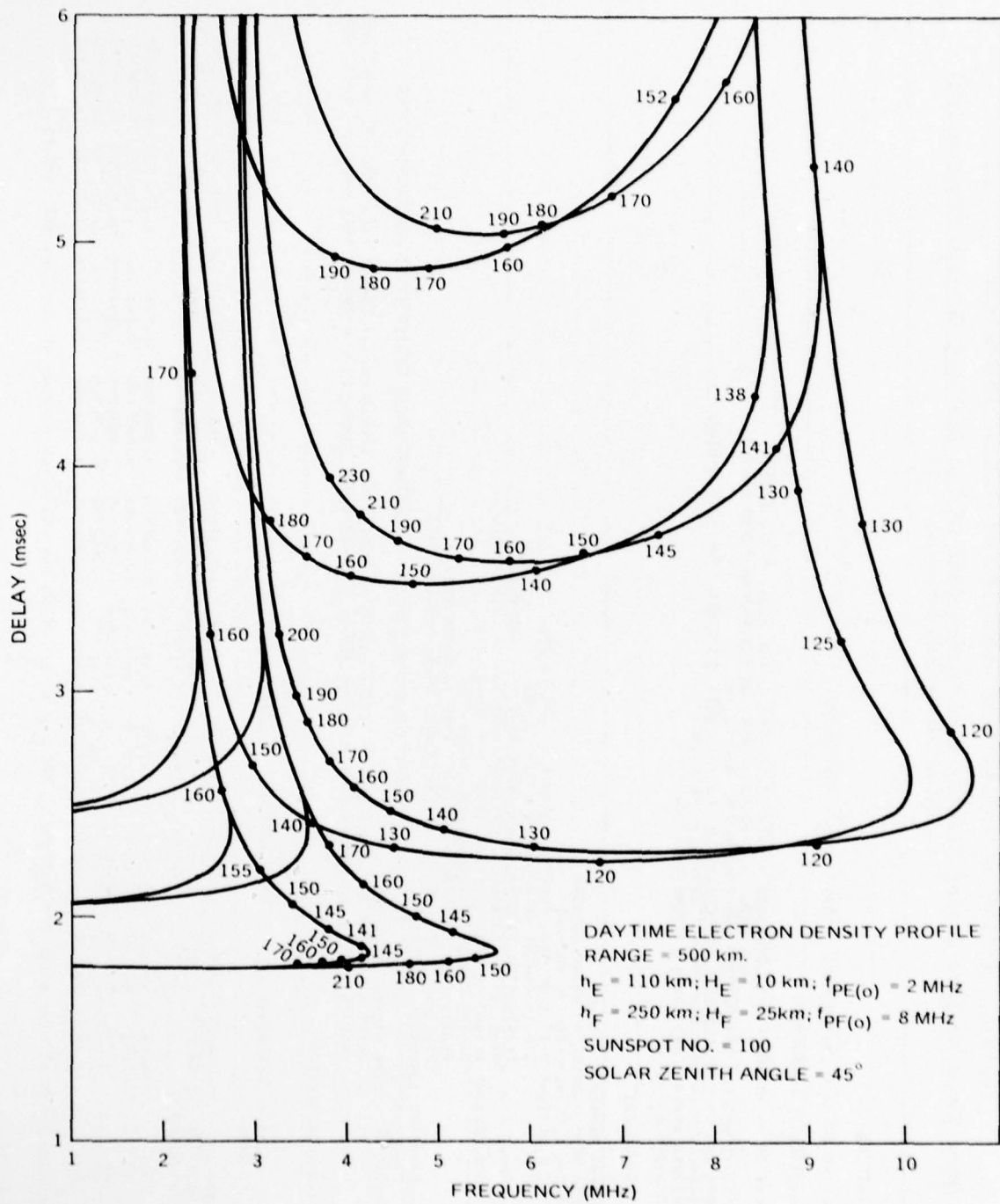


Figure 5. Computed Ionosphere Returns for One, Two and Three Hops
 (Numbers on Curves are Attenuation in dB)

IV. SIGNAL ANALYSIS

This section is concerned with the signal analysis part of the simulator and the approximations used in its implementation. We will assume that the transmitted signal, $s(t)$, is bandlimited with (two sided) bandwidth BW . The received signal, $r(t)$, is not strictly bandlimited because it is multiplied by the random gains, which are not bandlimited. However, since the doppler spreads are small compared with the signal bandwidth, the received signal can also be assumed to be bandlimited but with a slightly larger bandwidth than the transmitted signal. The error introduced by this assumption is negligible as long as the assumed bandwidth of the received signal is large compared with the sum of the transmitted signal bandwidth and the largest doppler spread present. In the following we will assume that all signals have a bandwidth equal to twice that of the transmitted signal. This is sufficient to reduce aliasing errors to a negligible value. Denoting the sampling interval associated with this larger bandwidth by T_o we have

$$T_o = \frac{1}{2 \cdot BW} \quad (50)$$

As a consequence of the cardinal series representation for band-limited functions, we require a knowledge of the signals involved only at the sample times nT_o , $n = 0, \pm 1, \dots$. This greatly simplifies the computational and storage requirements. From (21) the received, sampled signal appears as

$$r(nT_o) = A_g s(nT_o - N_o T_o) + \sum_{j=1}^N \exp[-2\pi i D_j^{(o)}] \cdot G_j(nT_o) \hat{s}_j(nT_o - N_j T_o) \quad n=0, 1, \dots \quad (51)$$

where the various delays have been replaced by the nearest integer multiple of T_o . That is, N_o is defined as the integer satisfying

$$D_g - \frac{1}{2} T_o \leq N_g T_o < D_g + \frac{1}{2} T_o \quad (52)$$

and the N_j 's are defined as the integers satisfying

$$D_j^{(1)} - \frac{1}{2} T_o \leq N_j T_o < D_j^{(1)} + \frac{1}{2} T_o, \quad j=1, \dots, N. \quad (53)$$

It remains to determine the sampled, distorted signals $\hat{s}_j(nT_o)$ and the sampled random path gains $G_j(nT_o)$.

A. Delay Distortion

The transmitted signal has the representation

$$s(t) = \sum_{n=-\infty}^{\infty} s(nT_o) \frac{\sin 2\pi BW(t-nT_o)}{2\pi BW(t-nT_o)} \quad (54)$$

and the impulse response $h_j(t)$, which we also assume to be band-limited, has the representation

$$h_j(t) = \sum_{n=-\infty}^{\infty} h_j(nT_o) \frac{\sin 2\pi BW(t-nT_o)}{2\pi BW(t-nT_o)}, \quad j=1, \dots, N. \quad (55)$$

We obtain the distorted waveform, $\hat{s}_j(t)$, by convolving $s(t)$ and $h_j(t)$. But $\hat{s}_j(t)$ also has an expansion of the above type and

$$\hat{s}_j(t) = \sum_{n=-\infty}^{\infty} \hat{s}_j(nT_o) \frac{\sin 2\pi BW(t-nT_o)}{2\pi BW(t-nT_o)}, \quad j=1, \dots, N. \quad (56)$$

We are interested here in the sample values $\hat{s}_j(nT_o)$ and these are given by the convolution

$$\hat{s}_j(nT_o) = \sum_{m=-\infty}^{\infty} s(nT_o - mT_o) \hat{h}_j(mT_o), \quad j=1, \dots, N. \quad (57)$$

where

$$\hat{h}_j(mT_0) = T_0 h_j(mT_0) = T_0 \int_{-BW}^{BW} H_j(f) \exp [2\pi ifmT_0] df. \quad (58)$$

$j=1, \dots, N$

The transfer function $H_j(f)$ is given by (11), and it will be approximated with the first two terms of the series appearing in the exponent, that is

$$H_j(f) \approx \exp[-2\pi if^2 D_j^{(2)} - 2\pi if^3 D_j^{(3)}], \quad j=1, \dots, N. \quad (59)$$

After the change of variable $\eta = f/BW$, we obtain from (58)

$$\hat{h}_j(mT_0) \approx \frac{1}{2} \int_{-1}^1 \exp[-i\Delta_j^{(2)} \eta^2 - i\Delta_j^{(3)} \eta^3] \cdot \exp[im\pi\eta] d\eta \quad (60)$$

$j=1, \dots, N$

with

$$\Delta_j^{(2)} = 2\pi (BW)^2 D_j^{(2)} \quad (61)$$

$$\Delta_j^{(3)} = 2\pi (BW)^3 D_j^{(3)}. \quad (62)$$

Closed form expressions for (60) are not known and further approximations are required for the numerical determination of $\hat{h}_j(mT_0)$. Let $I(x)$ represent the general integral defining the impulse responses, that is

$$I(x) = \frac{1}{2} \int_{-1}^1 \exp[-i\Delta^{(2)} \eta^2 - i\Delta^{(3)} \eta^3] \cdot \exp[ix\eta] d\eta. \quad (63)$$

Expanding $\exp[-i\Delta^{(3)} \eta^3]$ in a power series we have the representation

$$I(x) = \sum_{p=0}^{\infty} \frac{(-i\Delta^{(3)})^p}{p!} I_p(x) \quad (64)$$

where we have defined

$$I_p(x) = \frac{1}{2} \int_{-1}^1 \eta^{3p} \exp[-i\Delta^{(2)} \eta^2] \cdot \exp[ix\eta] d\eta \quad (65)$$

The integral $I_0(x)$ is readily expressed in terms of Fresnel integrals [24]. For the higher order integrals the following recurrence relation has been derived

$$I_p(x) = \frac{i}{4\Delta^{(2)}} \exp[-i\Delta^{(2)}] \left\{ \exp[ix] + (-1)^p \exp[-ix] \right\} \\ + \frac{x}{2\Delta^{(2)}} I_{p-1}(x) - i \frac{(p-1)}{2\Delta^{(2)}} I_{p-2}(x), \quad p \geq 1. \quad (66)$$

where we have adopted the convention that $I_{-1}(x) = 0$.

The impulse responses for the ionosphere returns can now be evaluated with relative ease. Starting with $I_0(x)$ and using (66) we determine as many of the terms $I_p(x)$ as are needed to adequately approximate the infinite sum (64). The integral $I_0(x)$ is evaluated using the rational approximation presented in [25]. Care must be exercised in implementing this procedure, however. The error incurred by using the rational approximation for $I_0(x)$ is approximately 1.0×10^{-9} . For large arguments ($x > 5$) nearly equal functions are subtracted in (66) and this reduces the number of significant figures in the resulting expression. For the higher order terms this reduction in the number of significant figures is important and the computed values may become inaccurate. It is evident from (64) that this effect will be more noticeable when $\Delta^{(3)}$ is large. Experience has shown that values of x as large as 20-25 can be tolerated in most applications before the errors become excessive.

B. Random Gains

The random gains, $G_j(t)$, in the ionosphere returns are complex valued, zero mean, Gaussian processes whose correlation function and power spectral density are given by (cf. Eqns. 19 and 20)

$$C_{G_j}(\tau) = A_j^2 \exp[-2\pi^2 \sigma_j^2 \tau^2 + 2\pi i v_j \tau] , j=1, \dots, N \quad (67)$$

and

$$P_{G_j}(f) = \frac{A_j^2}{\sqrt{2\pi}\sigma_j} \exp\left[-\frac{(f-v_j)^2}{2\sigma_j^2}\right] , j=1, \dots, N. \quad (68)$$

We wish to generate a random sequence with the above correlation function and we wish to do this directly in the time domain and not rely on Fourier transform techniques. Because the doppler spreads, σ_j , are small relative to the signal bandwidths, the time domain approach requires a large memory. To avoid these large memory requirements we will replace the original process with an approximation that can be generated more easily.

The approximate random gain will be denoted by $\tilde{G}_j(t)$ and it will be chosen to have the power spectral density

$$P_{\tilde{G}_j}^v(f) = \frac{8A_j^2}{3\pi\rho\sigma_j} \frac{1}{\left[1 + \left(\frac{f-v_j}{\rho\sigma_j}\right)^2\right]^3} , j=1, \dots, N \quad (69)$$

and corresponding correlation function

$$C_{\tilde{G}_j}^v(\tau) = A_j^2 \left[1 + 2\pi\rho\sigma_j|\tau| + \frac{1}{3}(2\pi\rho\sigma_j|\tau|)^2\right] \cdot \exp\left[-2\pi\rho\sigma_j|\tau| + 2\pi i v_j \tau\right] , j=1, \dots, N. \quad (70)$$

The parameter ρ is chosen so that (70) agrees with (67) over a reasonable range of arguments. The value $\rho = 2.1$ has been determined to be a good choice and this is the value that will be used

throughout the following. Normalized plots of $C_{G_j}(\tau)$ and $C_{G_j}^v(\tau)$ are compared in Figure 6.

It is obvious from (69) that the approximate process $\hat{G}_j(t)$ is not bandlimited. However, the error introduced by assuming that the process has bandwidth BW will be negligible since $(\sigma_j/BW) \ll 1$. Accordingly we will treat $\hat{G}_j(t)$ as if it is bandlimited, in which case we need only evaluate it at the sample times nT_o . Thus, the original problem has been reduced to the generation of a complex valued, zero mean, Gaussian sequence with correlation function

$$C_{G_j}^v(nT_o) = A_j^2 \left[1 + 2\pi\rho\sigma_j T_o |n| + \frac{1}{3} (2\pi\rho\sigma_j T_o |n|)^2 \right] \cdot \exp \left[-2\pi\rho\sigma_j T_o |n| + 2\pi i v_j T_o n \right] \quad (71)$$

$n=0, \pm 1, \dots$
 $j=1, \dots, N$

The technique used for the computer generation of the approximate process is discussed in Appendix C. A plot of the normalized, empirical correlation function of the computer-generated process is also displayed in Figure 6. Agreement between the computer-generated correlation function and the approximate correlation function (71) is excellent for the range of arguments considered.

C. Computer Program

A listing of the Fortran program used to implement the signal analysis part of the simulator is presented in Appendix D. Channel parameter information is read into the program via data cards that have been produced by the first part of the simulator. The sampled input values are read from a tape, the program calculates the sampled output values according to Eqn. (51) and writes the output on another tape. As an alternate, printed output also can be obtained, but, because the quantity of output data is large, the usefulness of this mode of presentation is severely limited.

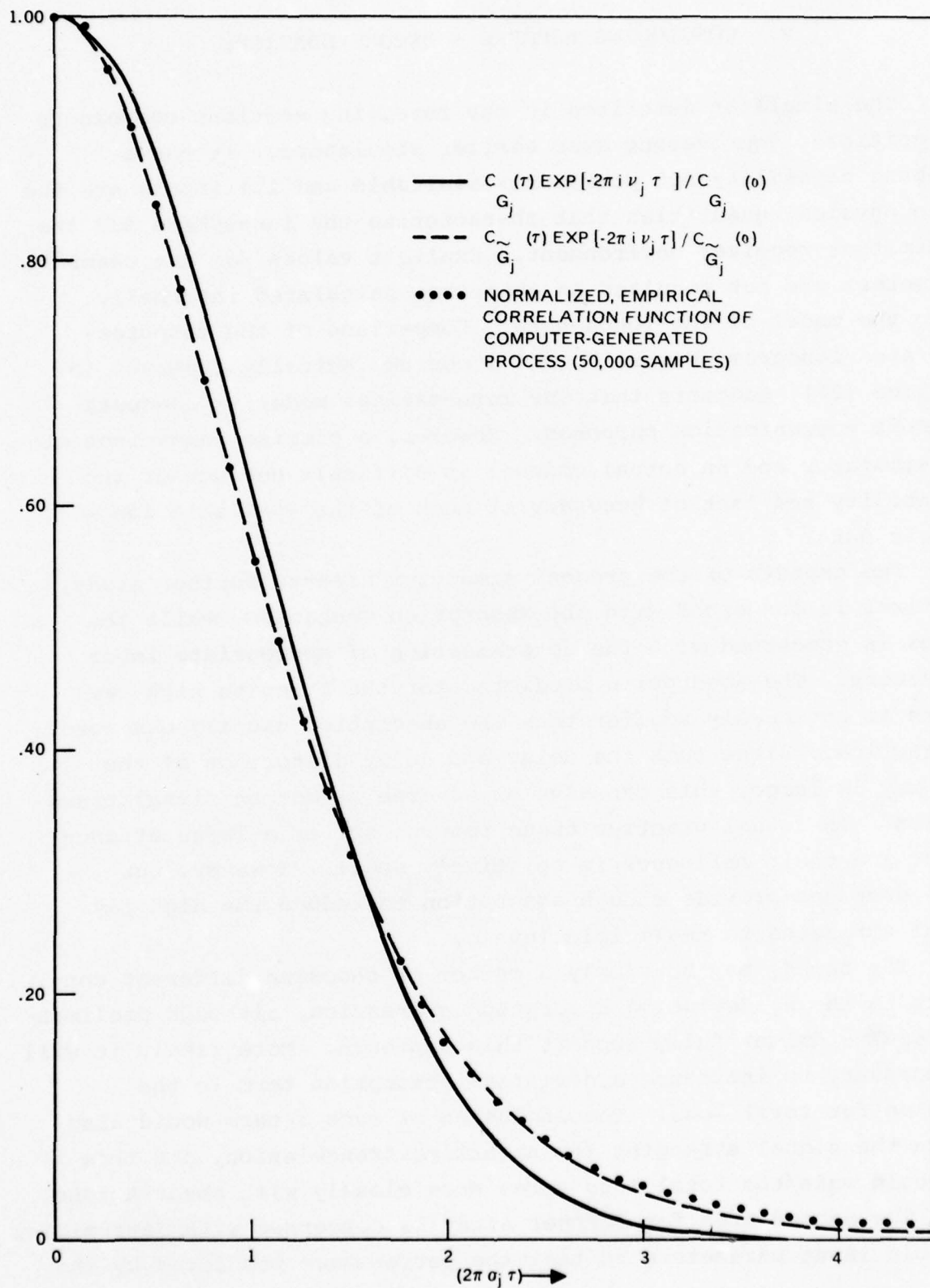


Figure 6. Normalized Correlation Function for the Random Gains

V. CONCLUDING REMARKS - RECOMMENDATIONS

The simulator described in the foregoing sections represents a significant improvement over earlier simulators. It has a wideband capability not previously available and its inputs are the basic physical quantities that characterize the ionosphere and the transmitter-receiver environment. Explicit values for the channel parameters are not required as these are calculated internally using the model of the ionosphere. Comparison of the computer-generated ionogram, Figure 5, and ionograms actually observed in practice [27], suggests that our mathematical model is adequate for most communication purposes. However, a precise comparison of the simulator and an actual channel is difficult because of the variability and lack of accuracy of much of the available ionospheric data.

Two aspects of the present simulator deserve further study. The first is concerned with the absorption mechanism, while the second is concerned with the determination of appropriate input parameters. The absorption predicted for the F region high ray return is noticeably smaller than the absorption usually observed in practice. Since both the delay and delay distortion of the high ray is large, this can have an adverse affect on signal transmission. In actual practice these returns suffer a large attenuation, and their influence is relatively small. However, our model does not provide enough absorption to reduce the high ray signal strengths to negligible levels.

The remedy may be simply a matter of choosing different constants in the nondeviative absorption expression, although preliminary results do not fully support this approach. More likely it will be necessary to introduce a deviative absorption term in the equation for total loss. The inclusion of such a term would also reduce the signal strengths for nighttime transmission, and this too would make the total loss agree more closely with observations.

The second area for further study is concerned with determining suitable input parameters so that the performance predicted by the

mathematical model agrees as well as possible with the actual observed performance. This involves matching actual and computer-generated observables such as doppler shift, doppler spread, attenuation and delay vs. frequency plots (ionograms) to determine the input parameters. Besides the obvious advantage of providing further justification of the assumptions used in the model, this parameter determination would provide the user with a set of inputs that correspond to a variety of actual environments.

The primary difficulty encountered in the determination of the input parameters is that an explicit functional relationship does not exist between the input parameters and the computed channel parameters; the channel parameters are determined by numerically solving a transcendental equation. As a consequence, techniques must be developed that are tailored to the ionosphere model. One approach is to select the most significant observable features and to determine the relationship between these features and the input parameters. For example, the nearly horizontal portions of an observed ionogram would be affected most by the heights of the regions and to a lesser degree by the thickness of the regions and their peak electron densities. On the other hand, the maximum operating frequency is likely to be more affected by the peak electron densities than the heights or thicknesses of the regions. A detailed study of these and other pertinent relationships would provide the user with the ability to determine input parameters corresponding to a variety of observed operating conditions. These same conditions could then be reproduced by the channel simulator as required for system studies.

VI REFERENCES

- [1] C.C. Watterson, J.R. Juroshek and W.D. Benesema, "Experimental Confirmation of an HF Channel Model," IEEE Transactions on Communication Technology, Vol. COM-18, pp. 792-803, 1970.
- [2] W.F. Walker, "Baseband Multipath Fading Simulator," Radio Science, Vol. 1, pp. 763-767, 1966.
- [3] R. Cole, W.M. Jewett and J.W. Linnehan, Jr., "A Programmable Real-Time HF Channel Simulator," Proceedings of the Sixth Annual Conference on Modeling and Simulation, pp. 259-266, 1975.
- [4] K.K. Clarke, "Random Channel Simulation and Instrumentation," IEEE Communications Convention Record, pp. 623-629, 1965.
- [5] D.B. Sailors and J.R. Hill, "Simulation and Measurement of High Frequency Ionospheric Channels," NOSC Technical Report 111, April 1977.
- [6] K.G. Gray and S.A. Bowhill, "The Impulse Response of a Cold Stratified Plasma in the Presence of Collisions and a Vertical Magnetic Field by a Multiple-Scattering Technique," Radio Science, Vol. 9, pp. 559-566, 1974.
- [7] K.G. Gray and S.A. Bowhill, "Transient Response of Stratified Media: Multiple-Scattering Integral and Differential Equations for an Impulsive Incident Plane Wave," Radio Science, Vol. 9, pp. 57-62, 1974.
- [8] K.G. Gray and S.A. Bowhill, "Transient Response of Stratified Media: Response to an Arbitrary Incident Plane Wave," Radio Science, Vol. 9, pp. 63-69, 1974.
- [9] K.G. Gray, "An Integral Equation for the Transient Response of a Stratified Magnetoplasma," IEEE Transactions on Antennas and Propagation, Vol.24, pp. 539-541, 1976.
- [10] D.A. Hill and J.R. Wait, "Theory of the Electromagnetic Transient Response of the Ionosphere for Plane Wave Excitation," Pure and Applied Geophysics, Vol. 90, pp. 169-186, 1971.
- [11] S.O. Rice, "Mathematical Analysis of Random Noise," Bell System Technical Journal, Vol.23, pp. 282-332 and Vol.24, pp. 46-156, 1944 and 1945.
- [12] H.N. Shaver, B.C. Tupper and J.B. Lomax, "Evaluation of a Gaussian HF Channel Model," IEEE Transactions on Communication Technology, Vol. COM-15, pp. 79-88, 1967.

- [13] J.T. Boys, "Statistical Variations in the Apparent Specular Component of Ionospherically Reflected Radio Waves," Radio Science, Vol. 3, pp. 984-990, 1968.
- [14] M. Balser and W.B. Smith, "Some Statistical Properties of Pulsed Oblique HF Ionospheric Transmissions," Journal of Research of the National Bureau of Standards, Vol. 66D, pp. 721-730, 1962.
- [15] D.E. Barrick, "Theory of Ground-Wave Propagation Across a Rough Sea at Dekameter Wavelengths," Battelle Memorial Institute Report, Contract DAAH01-70-C-0312, 1970.
- [16] K. Davies, Ionospheric Radio Propagation, National Bureau of Standards Monograph 80, U.S. Government Printing Office, Washington, D.C., 1965.
- [17] I.S. Gradshteyn and I.M. Ryzhik, Table of Integrals, Series and Products, Academic Press, New York, 1965.
- [18] R. A. Shepherd and J.B. Lomax, "Frequency Spread in Ionospheric Radio Propagation," IEEE Transactions on Communication Technology, Vol. COM-15, pp. 268-275, 1967.
- [19] P.A. Fialer, "Irregularities in the Quiet Ionosphere and their Effect on Propagation," Technical Report No. 156, Radio Science Laboratory, Stanford Electronics Laboratories, Stanford University, 1970.
- [20] W. Pfister, "The Wave-Like Nature of Inhomogeneities in the E-Region," Journal of Atmospheric and Terrestrial Physics, Vol. 33, pp. 999-1025, 1971.
- [21] F. David, A.G. Franco, H. Sherman and L.B. Shucavage, "Correlation Measurements on HF Transmission Link," IEEE Transactions on Communication Technology, Vol. COM-17, pp. 245-394, 1967.
- [22] K. Davies, "The Measurement of Ionospheric Drifts by Means of a Doppler Shift Technique," Journal of Geophysical Research, Vol. 67, pp. 4909-4913, 1962.
- [23] K. Davies and D.M. Baker, "On Frequency Variations of Ionospherically Propagated HF Radio Signals," Radio Science, Vol. 1, pp. 545-556, 1966.
- [24] M. Abramowitz and I.A. Stegun, Handbook of Mathematical Functions, National Bureau of Standards, Applied Mathematics Series No. 55, U.S. Government Printing Office, Washington, 1964.

- [25] J. Boersma, "Computation of Fresnel Integrals," Math. Comp., Vol. 14, p. 380, 1960.
- [26] E. Parzen, Stochastic Processes, Holden Day, San Francisco, 1962.
- [27] J.E. Hipp and T.C. Green, "Measured Sea Path Sky Wave/Ground Wave Signal Power Ratios over the 2-10 mHz Range," Southwest Research Institute Task Report XXXIII, Contract N00039-72-C-1275, Naval Electronic Systems Command, 1976.

APPENDIX A
DELAY AND DELAY DERIVATIVES

APPENDIX A
DELAY AND DELAY DERIVATIVES

In this appendix we present the equations for the delay and the first three delay derivatives. Recalling the definition of $A(x)$ we have

$$A(x) = 2G \left(\frac{1-x^2}{x} \right)^{\frac{1}{2}} \quad (\text{A.1})$$

where $x = \cos \theta$. We must solve the equation

$$R = A(x) \quad (\text{A.2})$$

with R equal to the distance between transmitter and receiver. The solution then yields the delay via the equation

$$\tau = \frac{R}{c(1-x^2)^{\frac{1}{2}}} \quad (\text{A.3})$$

with c the velocity of light. The delay derivatives are given by

$$\frac{d\tau}{df} = \frac{x\tau}{(1-x^2)} \frac{dx}{df} \quad (\text{A.4})$$

$$\frac{d^2\tau}{df^2} = \frac{1+2x^2}{x^2\tau} \left(\frac{d\tau}{dx} \right)^2 + \frac{x\tau}{(1-x^2)} \frac{d^2x}{df^2} \quad (\text{A.5})$$

and

$$\begin{aligned} \frac{d^3\tau}{df^3} = & - \frac{3(1+x^2+2x^4)}{x^4\tau^2} \left(\frac{d\tau}{df} \right)^2 + \frac{3(1+2x^2)}{x^2\tau} \left(\frac{d\tau}{df} \right) \left(\frac{d^2\tau}{df^2} \right) \\ & + \frac{x\tau}{(1-x^2)} \frac{d^3x}{df^3} \quad (\text{A.6}) \end{aligned}$$

Thus to determine the delay and delay derivatives we must solve (A.2) for x and then evaluate the first three derivatives of x with respect to f for use in (A.4) - (A.6). In the following these functions are listed for the two electron density profiles. The group height $G(x)$ is obtained by evaluating the integral (24).

1. Nighttime

For the nighttime electron density the integral for the group height is evaluated and used in (A.1) to yield

$$A(x) = \begin{cases} 2\left(\frac{1-x^2}{x^2}\right)^{\frac{1}{2}} \left\{ h_E - 2H_E + H_E \hat{f}_E x \ln \left(\frac{1+\hat{f}_E x}{1-\hat{f}_E x} \right) \right\}, & \hat{f}_E x \leq 1 \\ 2\left(\frac{1-x^2}{x^2}\right)^{\frac{1}{2}} \left\{ h_F - 2H_F - 4H_E + 2H_E \hat{f}_E x \ln \left(\frac{\hat{f}_E^{x+1}}{\hat{f}_E^{x-1}} \right) \right. \\ \left. + H_F \hat{f}_F x \ln \left(\frac{1+\hat{f}_F x}{1-\hat{f}_F x} \right) \right\}, & \hat{f}_E x > 1 \end{cases} \quad (A.7)$$

where

$$\hat{f}_E = \frac{f}{f_{pE}} \text{ and } \hat{f}_F = \frac{f}{f_{pF}} .$$

For $\hat{f}_E x \leq 1$ the derivatives of x with respect to frequency are:

$$\frac{dx}{df} = \left(\frac{x}{f}\right) \frac{R \cdot \left(\frac{x^2}{1-x^2}\right)^{\frac{1}{2}} - \left[2h_E - \frac{4H_E}{1-\hat{f}_E^2 x^2} \right]}{R \cdot \left(\frac{x^2}{1-x^2}\right)^{\frac{3}{2}} + \left[2h_E - \frac{4H_E}{1-\hat{f}_E^2 x^2} \right]}, \quad \hat{f}_E x \leq 1 \quad (A.8)$$

$$\frac{d^2x}{df^2} = \frac{1}{x} \left(\frac{dx}{df} \right)^2 - \frac{1}{f} \left(\frac{dx}{df} \right)$$

$$+ \frac{\left(\frac{x}{f} \right) \cdot \frac{R \cdot \left(\frac{1}{1-x^2} \right)^{3/2} \left(\frac{dx}{df} \right) \left[1 - \frac{3xf}{1-x^2} \frac{dx}{df} \right] + \frac{8H_E f \hat{f}_E^2 \left(\frac{x}{f} + \frac{dx}{df} \right)}{\left(1 - \hat{f}_E^2 x^2 \right)^2}}{R \cdot \left(\frac{x^2}{1-x^2} \right)^{3/2} + \left[2h_E - \frac{4H_E}{1 - \hat{f}_E^2 x^2} \right]}, \quad \hat{f}_E x < 1. \quad (A.9)$$

$$\frac{d^3x}{df^3} = -\frac{1}{x^2} \left(\frac{dx}{df} \right)^3 + \frac{2}{x} \left(\frac{dx}{df} \right) \left(\frac{d^2x}{df^2} \right) + \frac{1}{f^2} \left(\frac{dx}{df} \right) - \frac{1}{f} \left(\frac{d^2x}{df^2} \right)$$

$$- \frac{1}{x} \left(\frac{x}{f} - \frac{dx}{df} \right) \left[\frac{d^2x}{df^2} - \frac{1}{x} \left(\frac{dx}{df} \right)^2 + \frac{1}{f} \frac{dx}{df} \right]$$

$$- \frac{\left[\frac{d^2x}{df^2} - \frac{1}{x} \left(\frac{dx}{df} \right)^2 + \frac{1}{f} \frac{dx}{df} \right]}{R \cdot \left(\frac{x^2}{1-x^2} \right)^{3/2} + \left[2h_E - \frac{4H_E}{1 - \hat{f}_E^2 x^2} \right]} \left\{ \frac{3R \cdot x^2 \left(\frac{dx}{df} \right)}{\left(1-x^2 \right)^{5/2}} - \frac{8H_E x \hat{f}_E^2 \left(\frac{x}{f} + \frac{dx}{df} \right)}{\left(1 - \hat{f}_E^2 x^2 \right)^2} \right\}$$

$$+ \frac{\left(\frac{x}{f} \right)}{R \cdot \left(\frac{x^2}{1-x^2} \right)^{3/2} + \left[2h_E - \frac{4H_E}{1 - \hat{f}_E^2 x^2} \right]} \left\{ \frac{R}{\left(1-x^2 \right)^{5/2}} \left[1 - \frac{3xf}{1-x^2} \frac{dx}{df} \right] \right.$$

$$\cdot \left[3x \left(\frac{dx}{df} \right)^2 + \left(1-x^2 \right) \frac{d^2x}{df^2} \right]$$

$$- \frac{3Rf \left(\frac{dx}{df} \right)}{\left(1-x^2 \right)^{5/2}} \left[\frac{1+x^2}{1-x^2} \left(\frac{dx}{df} \right)^2 + \left(\frac{x}{f} \right) \frac{dx}{df} + x \frac{d^2x}{df^2} \right]$$

$$+ \frac{32H_E x f \hat{f}_E^4 \left(\frac{x}{f} + \frac{dx}{df} \right)^3}{\left(1 - \hat{f}_E^2 x^2 \right)^3}$$

$$+ \frac{8H_E \hat{f}_E^2 \left(\frac{x}{f} + \frac{dx}{df} \right)}{\left(1 - \hat{f}_E^2 x^2 \right)^2} \left[\frac{x}{f} + 5 \frac{dx}{df} + 2f \frac{d^2x}{df^2} \right] \left. \right\}, \quad \hat{f}_E x < 1. \quad (A.10)$$

For $\hat{f}_E x > 1$ these derivatives appear as

$$\frac{dx}{df} = \left(\frac{x}{f}\right) \cdot \frac{F \cdot \left(\frac{x^2}{1-x^2}\right)^{\frac{1}{2}} - \left[2h_F + \frac{8H_E}{\hat{f}^2 E x^2 - 1} - \frac{4H_F}{1 - \hat{f}^2 F x^2}\right]}{F \cdot \left(\frac{x^2}{1-x^2}\right)^{\frac{3}{2}} + \left[2h_F + \frac{8H_E}{\hat{f}^2 E x^2 - 1} - \frac{4H_F}{1 - \hat{f}^2 F x^2}\right]}, \quad \hat{f}_E x > 1 \quad (\text{A.11})$$

$$\frac{d^2x}{df^2} = \frac{1}{x} \left(\frac{dx}{df}\right)^2 - \frac{1}{f} \left(\frac{dx}{df}\right)$$

$$+ \left(\frac{x}{f}\right) \cdot \frac{R \cdot \left(\frac{dx}{df}\right) \left[1 - \frac{3xf}{1-x^2} \frac{dx}{df}\right] + \frac{16H_E f \hat{f}^2 E \left(\frac{x}{f} + \frac{dx}{df}\right)^2}{(\hat{f}^2 E x^2 - 1)^2} + \frac{8H_F f \hat{f}^2 F \left(\frac{x}{f} + \frac{dx}{df}\right)^2}{(1 - \hat{f}^2 F x^2)^2}}{R \cdot \left(\frac{x^2}{1-x^2}\right)^{\frac{3}{2}} + \left[2h_F + \frac{8H_E}{\hat{f}^2 E x^2 - 1} - \frac{4H_F}{1 - \hat{f}^2 F x^2}\right]}, \quad \hat{f}_E x > 1 \quad (\text{A.12})$$

$$\frac{d^3x}{df^3} = -\frac{1}{x^2} \left(\frac{dx}{df}\right)^3 + \frac{2}{x} \left(\frac{dx}{df}\right) \left(\frac{d^2x}{df^2}\right) + \frac{1}{f^2} \left(\frac{dx}{df}\right) - \frac{1}{f} \left(\frac{d^2x}{df^2}\right)$$

$$- \frac{1}{x} \left(\frac{x}{f} - \frac{dx}{df}\right) \left[\frac{d^2x}{df^2} - \frac{1}{x} \left(\frac{dx}{df}\right)^2 + \frac{1}{f} \frac{dx}{df}\right]$$

$$- \frac{\left[\frac{d^2x}{df^2} - \frac{1}{x} \left(\frac{dx}{df}\right)^2 + \frac{1}{f} \frac{dx}{df}\right]}{R \cdot \left(\frac{x^2}{1-x^2}\right)^{\frac{3}{2}} + \left[2h_F + \frac{8H_E}{\hat{f}^2 E x^2 - 1} - \frac{4H_F}{1 - \hat{f}^2 F x^2}\right]} \left\{ \frac{3R x^2 \left(\frac{dx}{df}\right)}{(1-x^2)^{\frac{1}{2}}}\right.$$

$$\left. - \frac{16H_E x \hat{f}^2 E \left(\frac{x}{f} + \frac{dx}{df}\right)}{(\hat{f}^2 E x^2 - 1)^2} - \frac{8H_F x \hat{f}^2 F \left(\frac{x}{f} + \frac{dx}{df}\right)}{(1 - \hat{f}^2 F x^2)^2}\right\}$$

$$\begin{aligned}
& + \frac{\frac{x}{\hat{f}}}{R \cdot \left(\frac{x^2}{1-x^2}\right)^{\frac{3}{2}} + \left[2h_F + \frac{8H_E}{\hat{f}^2 E x^2 - 1} - \frac{4H_F}{1-\hat{f}^2 F x^2}\right]} \\
& \cdot \left\{ \frac{R \cdot \left[1 - \frac{3xf}{1-x^2} \frac{dx}{df}\right]}{(1-x^2)^{\frac{5}{2}}} \left[3x \left(\frac{dx}{df}\right)^2 + (1-x^2) \left(\frac{d^2x}{df^2}\right)\right] \right. \\
& - \frac{3Rf \left(\frac{dx}{df}\right)}{(1-x^2)^{\frac{5}{2}}} \left[\frac{1+x^2}{1-x} \left(\frac{dx}{df}\right)^2 + \left(\frac{x}{\hat{f}}\right) \frac{dx}{df} + x \frac{d^2x}{df^2} \right] \\
& - \frac{64H_E x f \hat{f}^4_E \left(\frac{x}{\hat{f}} + \frac{dx}{df}\right)^3}{(\hat{f}^2 E x^2 - 1)^3} + \frac{32H_F x f \hat{f}^4_F \left(\frac{x}{\hat{f}} + \frac{dx}{df}\right)^3}{(1-\hat{f}^2 F x^2)^3} \\
& + \frac{16H_E \hat{f}^2_E \left(\frac{x}{\hat{f}} + \frac{dx}{df}\right) \left[\frac{x}{\hat{f}} + 5 \frac{dx}{df} + 2f \frac{d^2x}{df^2}\right]}{(\hat{f}^2 E x^2 - 1)^2} \\
& + \frac{8H_F \hat{f}^2_F \left(\frac{x}{\hat{f}} + \frac{dx}{df}\right) \left[\frac{x}{\hat{f}} + 5 \frac{dx}{df} + 2f \frac{d^2x}{df^2}\right]}{(1-\hat{f}^2 F x^2)^2}, \quad f_E x > 1. \quad (A.13)
\end{aligned}$$

2. Daytime

The daytime electron density profile differs from the nighttime profile only for heights greater than h_E . Thus the daytime equations for $\hat{f}_E < 1$ are the same as the nighttime equations. In this case

$$A(x) = \begin{cases} 2 \left(\frac{1-x^2}{x^2} \right)^{\frac{1}{2}} \left\{ h_E - 2H_E + H_E \hat{f}_E x \ln \left(\frac{1+\hat{f}_E x}{1-\hat{f}_E x} \right) \right\}, & \hat{f}_E x \leq 1 \\ 2 \left(\frac{1-x^2}{x^2} \right)^{\frac{1}{2}} \left\{ h_E - 2H_E + H_E \hat{f}_E x \ln \left(\frac{\hat{f}_E x + 1}{\hat{f}_E x - 1} \right) \right. \\ \quad + [h_F - h_E - 2H_F (1-r^2)^{\frac{1}{2}}] \left(\frac{\hat{f}_E^2 x^2}{\hat{f}_E^2 x^2 - 1} \right)^{\frac{1}{2}} \\ \quad \left. + 2H_F \hat{f}_F x \ln \left[\frac{(1-r^2)^{\frac{1}{2}} + (\hat{f}_F^2 x^2 - r^2)^{\frac{1}{2}}}{(1-\hat{f}_F^2 x^2)^{\frac{1}{2}}} \right] \right\}, & \hat{f}_E x > 1 \end{cases} \quad (A.14)$$

where

$$r^2 = \frac{f_{pE}^2}{f_{pF}^2}.$$

For $\hat{f}_E x \leq 1$ the derivatives of x with respect to frequency are given by (A.8) - (A.10). For $\hat{f}_E x > 1$ we have

$$\frac{dx}{df} = \left(\frac{x}{\hat{f}} \right) \frac{R \cdot \left(\frac{x^2}{1-x^2} \right)^{\frac{1}{2}} - B(x)}{R \cdot \left(\frac{x^2}{1-x^2} \right)^{\frac{3}{2}} + B(x)}, \quad \hat{f}_E x > 1 \quad (A.15)$$

with $B(x)$ defined by

$$B(x) = 2h_E + \frac{4H_E}{\hat{f}_E^2 x^2 - 1} + 2 \left(h_F - h_E - 2H_F \sqrt{1-r^2} \right) \cdot \left(\frac{\hat{f}_E^2 x^2}{\hat{f}_E^2 x^2 - 1} \right)^{\frac{3}{2}} \\ - \frac{4H_F \hat{f}_F^3 x^3}{\sqrt{1-r^2} (\hat{f}_F^2 x^2 - r^2)^{\frac{1}{2}} + (\hat{f}_F^2 x^2 - r^2)} - \frac{4H_F \hat{f}_F^3 x^3}{1 - \hat{f}_F^2 x^2} \quad (A.16)$$

$$\frac{d^2x}{df^2} = \frac{1}{x} \left(\frac{dx}{df} \right)^2 - \frac{1}{f} \frac{dx}{df}$$

$$+ \frac{R \left(\frac{x}{f} \right) \frac{dx}{df} \left[1 - \frac{3xf}{1-x^2} \frac{dx}{df} \right] - \left(\frac{x}{f} + \frac{dx}{df} \right) \frac{dB(x)}{df}}{R \cdot \left(\frac{x^2}{1-x^2} \right)^{3/2} + B(x)}, \quad \hat{f}_E x > 1 \quad (\text{A.17})$$

$$\frac{dB(x)}{df} = \left(\frac{x}{f} + \frac{dx}{df} \right) \cdot \left\{ \frac{8H_E \hat{f}_E^2 x}{(\hat{f}_E^2 x^2 - 1)^2} - 6(h_F - h_E - 2H_F \sqrt{1-r^2}) \frac{\hat{f}_E^3 x^2}{(\hat{f}_E^2 x^2 - 1)^{5/2}} \right.$$

$$- \frac{12H_F \hat{f}_F^3 x^2}{\sqrt{1-r^2} (\hat{f}_F^2 x^2 - r^2)^{1/2} + (\hat{f}_F^2 x^2 - r^2)}$$

$$+ \frac{4H_F \hat{f}_F^5 x^4 \left[2 + \sqrt{1-r^2} (\hat{f}_F^2 x^2 - r^2)^{-1/2} \right]}{\left[\sqrt{1-r^2} (\hat{f}_F^2 x^2 - r^2)^{1/2} + (\hat{f}_F^2 x^2 - r^2) \right]^2}$$

$$- \frac{4H_F \hat{f}_F^3 x^2 (3 - \hat{f}_F^2 x^2)}{(1 - \hat{f}_F^2 x^2)^2} \left. \right\} \quad (\text{A.18})$$

$$\begin{aligned}
\frac{d^3 x}{df^3} = & -\frac{1}{x^2} \left(\frac{dx}{df} \right)^3 + \frac{2}{x} \left(\frac{dx}{df} \right) \left(\frac{d^2 x}{df^2} \right) + \frac{1}{f^2} \frac{dx}{df} - \frac{1}{f} \frac{d^2 x}{df^2} \\
& + \frac{1}{R \cdot \left(\frac{x^2}{1-x^2} \right)^{3/2} + B(x)} \left\{ -\frac{3R x \left(\frac{dx}{df} \right)}{(1-x^2)^{5/2}} \left[\frac{1+4x^2}{1-x^2} \left(\frac{dx}{df} \right)^2 + \left(\frac{x}{f} \right) \left(\frac{dx}{df} \right) + 3x \frac{d^2 x}{df^2} \right] \right. \\
& + \frac{R}{f \cdot (1-x^2)^{3/2}} \left[\frac{1+2x^2}{1-x^2} \left(\frac{dx}{df} \right)^2 - \left(\frac{x}{f} \right) \frac{dx}{df} + x \frac{d^2 x}{df^2} \right] \\
& - \frac{1}{f} \frac{dB(x)}{df} \left[2 \frac{dx}{df} - \frac{x}{f} + 2f \frac{d^2 x}{df^2} - \frac{f}{x} \left(\frac{dx}{df} \right)^2 \right] \\
& \left. - \left(\frac{x}{f} + \frac{dx}{df} \right) \frac{d^2 B(x)}{df^2} \right\}, \quad \hat{f}_E x > 1 \tag{A.19}
\end{aligned}$$

$$\begin{aligned}
\frac{d^2 B(x)}{df^2} = & \frac{1}{f} \frac{dB(x)}{df} \left[\frac{dx}{df} - \frac{x}{f} + f \frac{d^2 x}{df^2} \right] \\
& + \left(\frac{x}{f} + \frac{dx}{df} \right) \left\{ -\frac{8H_E \hat{f}^2 E}{(\hat{f}^2 E x^2 - 1)^3} \left[\hat{f}^2 E x^2 \left(2 \frac{x}{f} + 3 \frac{dx}{df} \right) + 2 \left(\frac{x}{f} + \frac{dx}{df} \right) \right] \right. \\
& \left. + \frac{6\hat{f}^3 E x (h_F - h_E - 2H_F \sqrt{1-r^2})}{(\hat{f}^2 E x^2 - 1)^{3/2}} \left[\hat{f}^2 E x^2 \left(2 \frac{x}{f} + 3 \frac{dx}{df} \right) + \left(3 \frac{x}{f} + 2 \frac{dx}{df} \right) \right] \right\}
\end{aligned}$$

$$\begin{aligned}
& + \frac{12H_F \hat{f}_F^3 x \left[-\left(3 \frac{x}{f} + 2 \frac{dx}{df}\right) + \hat{f}_F^2 x^2 \left(\frac{x}{f} + \frac{dx}{df}\right) \right] \left[2 + \sqrt{1-r^2} (\hat{f}_F^2 x^2 - r^2)^{-\frac{1}{2}} \right]}{\sqrt{1-r^2} (\hat{f}_F^2 x^2 - r^2)^{\frac{1}{2}} + (\hat{f}_F^2 x^2 - r^2)} \\
& + \frac{4H_F \hat{f}_F^5 x^3 \left(5 \frac{x}{f} + 4 \frac{dx}{df}\right) \left[2 + \sqrt{1-r^2} (\hat{f}_F^2 x^2 - r^2)^{-\frac{1}{2}} \right]}{\left[\sqrt{1-r^2} (\hat{f}_F^2 x^2 - r^2)^{\frac{1}{2}} + (\hat{f}_F^2 x^2 - r^2) \right]^2} \\
& - \frac{4H_F \hat{f}_F^7 x^5 \sqrt{1-r^2} \left(\frac{x}{f} + \frac{dx}{df}\right) \cdot (\hat{f}_F^2 x^2 - r^2)^{-\frac{3}{2}}}{\left[\sqrt{1-r^2} (\hat{f}_F^2 x^2 - r^2)^{\frac{1}{2}} + (\hat{f}_F^2 x^2 - r^2) \right]^2} \\
& - \frac{8H_F \hat{f}_F^7 x^5 \left(\frac{x}{f} + \frac{dx}{df}\right) \left[2 + \sqrt{1-r^2} (\hat{f}_F^2 x^2 - r^2)^{-\frac{1}{2}} \right]^2}{\left[\sqrt{1-r^2} (\hat{f}_F^2 x^2 - r^2)^{\frac{1}{2}} + (\hat{f}_F^2 x^2 - r^2) \right]^3} \\
& - \frac{16H_F \hat{f}_F^5 x^3 \left(\frac{x}{f} + \frac{dx}{df}\right) (3 - \hat{f}_F^2 x^2)}{(1 - \hat{f}_F^2 x^2)^3} \\
& - \frac{4H_F \hat{f}_F^3 x \left[3 \left(3 \frac{x}{f} + 2 \frac{dx}{df}\right) - \hat{f}_F^2 x^2 \left(5 \frac{x}{f} + 4 \frac{dx}{df}\right) \right]}{(1 - \hat{f}_F^2 x^2)^2} \left. \right\} \tag{A.20}
\end{aligned}$$

APPENDIX B
PROGRAM FOR CALCULATING CHANNEL PARAMETERS

START OF SEGMENT 002
 FORMAT SEGMENT IS 0002 LONG
 FORMAT SEGMENT IS 0000 LONG
 FORMAT SEGMENT IS 0005 LONG

DIMENSION T(40,14),P(4,8),AL(3)
 COMMON NE,HEM,HF,HFM,TIME

THIS PROGRAM COMPUTES CHANNEL PARAMETERS FROM BASIC INPUTS

GLOSSARY OF MOST IMPORTANT VARIABLES

- C C = CARRIER FREQUENCY (MHZ)
- C BW = BANDWIDTH (KHZ)
- C XLONG = LONGITUDE OF TRANSMITTER (DEGREES) + FOR WEST
 - FOR EAST
- C XLAT = LATITUDE OF TRANSMITTER (DEGREES) + FOR NORTH
 - FOR SOUTH
- C R = DISTANCE BETWEEN TRANSMITTER AND RECEIVER (KM)
- C RAG = DIRECTION FROM TRANSMITTER TO RECEIVER (DEGREES)
 MEASURED IN GEOGRAPHIC COORDINATES
- C RAM = DIRECTION FROM TRANSMITTER TO RECEIVER (DEGREES)
 MEASURED IN MAGNETIC COORDINATES
- C ISEA = SEA STATE
- C SPT = SUNSPOT NUMBER
- C ZEN = SOLAR ZENITH ANGLE (DEGREES)
- C TIME = TIME OF DAY ('DAY' OR 'NITE')
- C HEM = HEIGHT OF MAX. ELECTRON DENSITY IN E REGION (KM)
- C HFM = HEIGHT OF MAX. ELECTRON DENSITY IN F REGION (KM)
- C HMF = THICKNESS OF F REGION (KM)
- C FPEF = PENETRATION FREQ. OF F REGION U-WAVE (MHZ)
- C FPEX = PENETRATION FREQ. OF F REGION X-WAVE (MHZ)
- C FPIX = PENETRATION FREQ. OF F REGION A-WAVE (MHZ)
- C ABSML = MULTIPLICATIVE CONST. FOR NONDEVIATIVE ABSORPTION
- C SPTML = SUNSPOT NO. MULTIPLIER FOR NONDEVIATIVE ABSORPTION
- C SULXP = SOLAR ZFN. ARG. EXPNT. FOR NONDEVIATIVE ABSORPTION
- C SHIFLE = E REGION REFERENCE DOPPLER SHIFT (HZ)
- C EXSHTE = E REGION DOPPLER SHIFT EXPONENT
- C SPMDL = E REGION REFERENCE DOPPLER SPREAD (HZ)
- C EXSPRE = E REGION DOPPLER SPREAD EXPONENT
- C RFRFL = E REGION DOPPLER REFERENCE FREQ. (MHZ)
- C SHIFLF = F REGION REFERENCE DOPPLER SHIFT (HZ)
- C EXSHIF = F REGION DOPPLER SHIFT EXPONENT
- C SPRDF = F REGION REFERENCE DOPPLER SPREAD (HZ)
- C EXSPRF = F REGION DOPPLER SPREAD EXPONENT
- C RFRWF = F REGION DOPPLER REFERENCE FREQ. (MHZ)
- C ATT = ATTENUATION (DB)
- C ATTDIF = ATTENUATION DIFFERENCE BETWEEN STRONGEST RETURN
 FROM IONOSPHERE AND WEAKEST RETURN RETAINED
- C NPATR = NO. OF TROPOSPHERE REFLECTIONS RETAINED
- C GDELAY = GROUNDWAVE DELAY (SEC)
- C GATTEN = GROUNDWAVE ATTENUATION (DB)
- C TPUNCH = PRINT SELECTOR FOR TCIJ ARRAY ('ALL' OR 'NET')
- C HPUNCH = PUNCH SELECTOR PUNCHES DATA CARDS FOR USE IN
 SIGNAL ANALYSIS PART OF SIMULATOR IF NPUNCH=1,
 DJFS NOT PUNCH DATA CARDS IF NPUNCH=0.
- C ARRAY T(I,J) CONTAINS THE FOLLOWING PARAMETERS

```

C      I = NI INDEX NUMBER FOR PATH
C      J = IF NUMBER OF HOPS
C      K = 2: REGION AND MAGNETIOMIC INDICATOR (EO = E REGION =
C      L: ORDINARY WAVES) SIMILARLY FOR EX, FO, AND FX)
C      M: 'HIGH' (FOR HIGH RAY) OR 'LOW' (FOR LOW RAY)
C      N: SOLUTION INDICATOR (MENU SOLUTION, I=SOLUTION)
C      O: 5: THETA = RAY ANGLE MEASURED FROM VERTICAL (DEGREES)
C      P: 6: PATH LENGTH (KM)
C      Q: 7: DELAY AT CARRIER FREQUENCY (SEC)
C      R: 8: RECEIVED CARRIER PHASE (CYCLES)
C      S: 9: SIGNAL DELAY (SEC)
C      T: 10: AMPLITUDE DISTORTION (SEC/MHZ)
C      U: 11: PHASE DISTORTION (SEC/MHZ**2)
C      V: 12: ATTENUATION (DB)
C      W: 13: DOPPLER SHIFT (HZ)
C      X: 14: DOPPLER SPREAD (HZ)

C      PIWJ.IIIS9265359
C      TMS'NITL'
C      PRF'PRET'
C      READ DATA
C      READ/2/7/5/BH
C      READ/2/XLONGPXLAT
C      READ/2/R
C      READ/2/RNG
C      READ/2/SEA
C      READ/2/SPT
C      READ/2/ZEN
C      READ/2/AVOYTIME
C      READ/2/HEM/HEFPEU
C      READ/2/HFHF/FPFU
C      READ/2/AS/SLT/SP/MLT/SOLEXP
C      READ/2/SMIT/FE/EX/STB/SP/PROF/EX/SPRT/RF/RF/RF
C      READ/2/SMIT/EX/SHTR/SP/ROF/EX/SPRT/RF/RF/RF
C      READ/2/ATTOIF
C      READ/2/GUELAY/UALIEM
C      READ/2/VOO/TP/IRI
C      READ/2/MPUNCH
C      END READ DATA
C      COMPUTE PENETRATION FREQUENCIES FOR EXTRAORDINARY WAVES
C      CALL GETMAG(XLAT,XLONG,XLATM,XLONGM)
C      SINPHI=IN(PI/180)*X(LATM)
C      XPHI=ASIN(SIN(180*(X(LONGM)-X(LONGM0))/180))
C      FPEX=XLAT*(16370/(16370+HEM))**3
C      FPEX=XLAT*(16370/(16370+HEM))**3
C      FPEX=5*FHEX*SWR((FPEX**2)+(25*(FHEX**2)))
C      FPEX=5*FHEX*SWR((FPEX**2)+(25*(FHEX**2)))
C      END COMPUTATION OF PENETRATION FREQS FOR EXTRAORDINARY WAVES
C      COMPUTE BEARING OF RECEIVER IN MAGNETIC COORDINATES
C      CALL RMGMAG(XLAT,XLONG,M,RAG,RAM)
C      WRTTF(6,910)
C      END COMPUTATION OF RECEIVER BEARING
C      WRTTF(6,911)
C      WRTTF(6,912)FC/BW
C      WRTTF(6,913)
C      WRTTF(6,915)XLONG
C      WRTTF(6,916)XLAT
C      WRTTF(6,917)H

```


909 FURMAT(6) 021034113
 910 FURMAT(6X)'SUMMARY OF TRANSMISSION PARAMETERS'/// 021034113
 911 FURMAT(1X)'SIGNAL PARAMETERS'// 021034113
 912 FURMAT(2X)'CARRIER FREQ. =',F7,2,' MHZ. BANDWIDTH =',F7,2,' KHZ 021034113
 1.) 021034113
 913 FURMAT(4X)'TRANSMITTER/RECEIVER PARAMETERS'// 021034113
 914 FURMAT(4X)'LOCATION OF TRANSMITTER LONGITUDE =',F7,2,' DEGREES (021034113
 1.) FOR WEST = FOR EAST'// 021034113
 915 FURMAT(4X)'LATITUDE =',F7,2,' DEGREES (1.) FOR NORTH = FOR SOUTH 021034113
 1.) 021034113
 916 FURMAT(4X)'DISTANCE BETWEEN TRANSMITTER AND RECEIVER =',F8,2,' KM. 021034113
 1.) 021034113
 917 FURMAT(4X)'DIRECTION FROM TRANSMITTER TO RECEIVER =',F6,2,' DEGREE 021034113
 1.) (MEASURED FROM TRUE NORTH) 021034113
 918 FURMAT(4X)'TRANSMITTER ANTENNA PATTERN = (3/2)*(SIN(THETA))**2'// 021034113
 919 FURMAT(4X)'RECEIVER ANTENNA PATTERN = (3/2)*(SIN(THETA))**2'// 021034113
 920 FURMAT(4X)'SEA STATE =',F7,2,' 021034113
 921 FURMAT(4X)'IONOSPHERE PARAMETERS'// 021034113
 922 FURMAT(4X)'SUNSPOT NUMBER =',F7,2,' 021034113
 923 FURMAT(4X)'DAYTIME ELECTRON DENSITY PROFILE'// 021034113
 924 FURMAT(4X)'NIGHTTIME ELECTRON DENSITY PROFILE'// 021034113
 925 FURMAT(4X)'HEIGHT OF MAX. ELECTRON DENSITY =',F7,2,' KM 021034113
 1.) 021034113
 926 FURMAT(25X)'PENETRATION FREQUENCY, EXTRAORDINARY WAVE =',F7,2,' MH 021034113
 12.) 021034113
 927 FURMAT(4X)'SOLAR ZENITH ANGLE =',F7,2,' DEGREES'// 021034113
 928 FURMAT(4X)'SOLAR ZENITH ANGLE = NOT APPLICABLE TO NIGHTTIME TRANSM 021034113
 929 FURMAT(4X)'SOLAR ZENITH ANGLE = NOT APPLICABLE TO NIGHTTIME TRANSM 021034113
 1.) ISSIUM'// 021034113
 930 FURMAT(1X)'COMPUTED CHANNEL PARAMETERS'// 021034113
 931 FURMAT(1X)'GROUNDWAVE DELAY =',F10,3,' SEC. ATTENUATION = 021034113
 1.) F10.3' DB.'// 021034113
 932 FURMAT(1X)'IONOSPHERE RETURN'// 021034113
 933 FURMAT(1X)'SIGNAL =',F7,2,' DB.'// 021034113
 934 FURMAT(1X)'SIGNAL =',F7,2,' DB.'// 021034113
 935 FURMAT(1X)'SIGNAL =',F7,2,' DB.'// 021034113
 936 FURMAT(1X)'SIGNAL =',F7,2,' DB.'// 021034113
 937 FURMAT(1X)'SIGNAL =',F7,2,' DB.'// 021034113
 938 FURMAT(1X)'SIGNAL =',F7,2,' DB.'// 021034113
 939 FURMAT(1X)'SIGNAL =',F7,2,' DB.'// 021034113
 940 FURMAT(1X)'SIGNAL =',F7,2,' DB.'// 021034113
 941 FURMAT(1X)'SIGNAL =',F7,2,' DB.'// 021034113
 942 FURMAT(1X)'SIGNAL =',F7,2,' DB.'// 021034113
 943 FURMAT(1X)'SIGNAL =',F7,2,' DB.'// 021034113
 944 FURMAT(1X)'SIGNAL =',F7,2,' DB.'// 021034113
 945 FURMAT(1X)'SIGNAL =',F7,2,' DB.'// 021034113
 946 FURMAT(1X)'SIGNAL =',F7,2,' DB.'// 021034113
 947 FURMAT(1X)'SIGNAL =',F7,2,' DB.'// 021034113
 948 FURMAT(1X)'SIGNAL =',F7,2,' DB.'// 021034113
 949 FURMAT(1X)'SIGNAL =',F7,2,' DB.'// 021034113
 950 FURMAT(1X)'SIGNAL =',F7,2,' DB.'// 021034113
 951 FURMAT(1X)'SIGNAL =',F7,2,' DB.'// 021034113
 952 FURMAT(1X)'SIGNAL =',F7,2,' DB.'// 021034113
 953 FURMAT(1X)'SIGNAL =',F7,2,' DB.'// 021034113

954 FURMAT(15X,'MULTIPLICATIVE CONSTANT *',F6.6,'',SUNSPOT NUMBER MULT
 IPLTR *',F6.6,'',SULAR ZENITH ANGLE EXPONENT *',F6.3)
 955 FURMAT(11,A2,A4,4E16.9)
 956 FURMAT(4E16.9)
 957 FURMAT(4E16.9)
 \$10\$
 END
 0021035213 IS THE LOCATION FOR EXCEPTIONAL ACTION ON THE I/O STATEMENT AT 0021000A0
 0021035215 IS THE LOCATION FOR EXCEPTIONAL ACTION ON THE I/O STATEMENT AT 0021000VC
 0021035217 IS THE LOCATION FOR EXCEPTIONAL ACTION ON THE I/O STATEMENT AT 0021000VA
 0021035219 IS THE LOCATION FOR EXCEPTIONAL ACTION ON THE I/O STATEMENT AT 0021000BA
 0021035221 IS THE LOCATION FOR EXCEPTIONAL ACTION ON THE I/O STATEMENT AT 00210007A
 0021035223 IS THE LOCATION FOR EXCEPTIONAL ACTION ON THE I/O STATEMENT AT 00210006B
 0021035225 IS THE LOCATION FOR EXCEPTIONAL ACTION ON THE I/O STATEMENT AT 00210005A
 0021035227 IS THE LOCATION FOR EXCEPTIONAL ACTION ON THE I/O STATEMENT AT 00210004D
 0021035229 IS THE LOCATION FOR EXCEPTIONAL ACTION ON THE I/O STATEMENT AT 00210003D
 0021035231 IS THE LOCATION FOR EXCEPTIONAL ACTION ON THE I/O STATEMENT AT 002100035
 0021035233 IS THE LOCATION FOR EXCEPTIONAL ACTION ON THE I/O STATEMENT AT 00210002U
 0021036211 IS THE LOCATION FOR EXCEPTIONAL ACTION ON THE I/O STATEMENT AT 002100025
 0021036213 IS THE LOCATION FOR EXCEPTIONAL ACTION ON THE I/O STATEMENT AT 00210001D
 0021036215 IS THE LOCATION FOR EXCEPTIONAL ACTION ON THE I/O STATEMENT AT 002100013
 0021036217 IS THE LOCATION FOR EXCEPTIONAL ACTION ON THE I/O STATEMENT AT 002100009

SECRET 002 IS 03CF LUNG

START OF SEGMENT 013

```

SURROUTIME PA(=C,FPE,FPE,FPE,FPE)
COMMONL, MEM, N, M, M, TIME
DIMENSIONP(0:0)

C EVALUATES ANGLE, PATH DISTANCE, DELAY AND DELAY DERIVATIVES
C FOR E REGION AND F REGION
C AHE = THICKNESS OF E REGION (KM)
C HEM = HEIGHT OF MAX. ELECTRON DENSITY IN E REGION (KM)
C FPE = PENETRATION FREQUENCY OF E REGION (MHZ)
C AHF = THICKNESS OF F REGION (KM)
C HFM = HEIGHT OF MAX. ELECTRON DENSITY IN F REGION (KM)
C FPF = PENETRATION FREQUENCY OF F REGION (MHZ)
C TIME = TIME OF DAY ('DAY' ON 'NITE')
C R = LENGTH OF GROUND PATH (KM)
C F = FREQUENCY (MHZ)
C X = COS(THETA), THETA=RAY ANGLE MEASURED FROM VERTICAL
C SURROUTIME RETURNS P(T,J)
C I = 1: LOW RAY, F REGION
C J = 2: HIGH RAY, F REGION
C J = 3: HIGH RAY, E REGION
C J = 4: LOW RAY, E REGION
C J = 5: SOLUTION INDICATOR (0=NO SOLUTION, 1=SOLUTION)
C J = 2: LENGTH OF GROUND PATH (KM)
C J = 3: COS(THETA)
C J = 4: LENGTH OF SIGNAL PATH (KM)
C J = 5: 1: PATH DELAY (SEC)
C J = 6: 1: DERIVATIVE OF DELAY (SEC/MHZ)
C J = 7: 2: SECOND DERIVATIVE OF DELAY (SEC/MHZ**2)
C J = 8: 3: THIRD DERIVATIVE OF DELAY (SEC/MHZ**3)

FNEF/FPE
FNF/FPF
TF(FNE=1, T0, T0, 20)
10 XMIN=1
P(2, J) = 0
P(3, J) = 0
P(4, J) = 0
13 CONTINUE
GOTO 40

C NO 30 OF LHMINS MINIMUM VALUE OF AE(X)

20 XLAST=1-E=10
CALL AE(FPE, P, XLAST, ATAST)
D30L=1.9
DIFF=1/(10.8*E)
26 XMIN=XLAST+DIFF
TF(FNF=1, XMIN, T0, 20, 20)
27 CALL AE(FPE, P, XMIN, PAMIN)
TF(FMIN=1, XLAST, T0, 20, 20)
28 XLAST=XMIN
ATAST=XMIN
GOTO 26
29 TFC=1336.36237
30 XLAST=XMIN+DIFF
GOTO 34
37 XLAST=XMIN+2*DIFF
38 CALL AE(FPE, P, XLAST, ATAST)

```



```

90 X4T=1.
   D95J=1.8
   P(4,2)=.
95 CONTINUE
   GOTO120
C
   DO 110 N,MIN,MAX
      XLAST=(L+R)/2
      CALL AF(FPE,FPP,F,ALAST,ALAST)
      DIF1=(L+R)/2
      DIF2=(L+R)/2
104 X4T=XLAST+DIF1
      IF(X4T-AMIN<1)GOTO109,109
107 CALL AF(FPE,FPP,F,AMIN,AMIN)
      IF(AMIN-ALAST)GOTO109,109
108 XLAST=AMIN
      ALAST=AMIN
      GOTO104
109 IF(L-1)GOTO116,116,117
116 XLAST=AMIN-DIFF
      GOTO116
117 XLAST=AMIN+2*DIFF
118 CALL AF(FPE,FPP,F,ALAST,ALAST)
119 CONTINUE
C
      IF MIN, AF(X), .GT., R, THERE ARE NO RETURNS FROM F REGION
111 DIF1=(L+R)/2
      P(3,2)=.
      P(4,2)=.
115 CONTINUE
      GOTO200
C
   DO 130 N,MIN,MAX
      XLAST=(L+R)/2
      DIF1=(L+R)/2
      DIF2=(L+R)/2
124 X=XLAST+DIF1
      IF(X-AMIN)GOTO127,129,129
127 CALL AF(FPE,FPP,F,ALAST,ALAST)
      IF(A-R)GOTO129,129,128
128 XLAST=X
      GOTO126
129 X=XLAST-DIFF
130 CONTINUE
      P(3,2)=.
      P(4,2)=.
      X=AMIN+(X+L)/2
      P(3,2)=.
      P(4,2)=.
      CALL DELAY(CRFFPE,FPP,F,ALAST,ALAST)
      P(3,2)=.
      P(4,2)=.
      P(3,2)=.
      P(4,2)=.
      IF(FNF=1)GOTO,200,200,140

```


APPENDIX C
COMPUTER GENERATION OF RANDOM GAINS

APPENDIX C
COMPUTER GENERATION OF RANDOM GAINS

For each ionosphere return, it is desired to generate a stationary, zero-mean Gaussian sequence $\hat{G}_j(nT_0)$, $n = 0, 1, \dots$, having the correlation function

$$\begin{aligned} C_{\hat{G}_j}(nT_0) &= E \hat{G}_j(nT_0 + mT_0) \hat{G}_j^*(mT_0) \\ &= A_j^2 \left[1 + (2\pi\rho\sigma_j T_0 |n|) + \frac{1}{3} (2\pi\rho\sigma_j T_0 |n|)^2 \right] \\ &\quad \cdot \exp \left[-2\pi\rho\sigma_j T_0 |n| + 2\pi i v_j T_0 n \right] \end{aligned} \quad (C.1)$$

$$\begin{aligned} n &= 0, 1, \dots \\ j &= 1, \dots, N. \end{aligned}$$

We will generate this sequence by passing a white noise process through an appropriately chosen discrete-time linear filter [26]. Denoting the filter input by $\{\xi_j(n)\}$ and the impulse response by $\{a_j(n)\}$ we have

$$\hat{G}_j(nT_0) = \exp[2\pi i v_j n T_0] \sum_{m=0}^{\infty} \xi_j(n-m) a_j(m) \quad (C.2)$$

$j=1, \dots, N$

where

$$a_j(m) = \begin{cases} A_j \left(\frac{8}{3} \pi \rho \sigma_j T_0 \right)^{\frac{1}{2}} (2\pi \rho \sigma_j m T_0)^2 \exp \left[-2\pi \rho \sigma_j m T_0 \right], & m \geq 0 \\ 0, & m < 0 \end{cases}, \quad j=1, \dots, N. \quad (C.3)$$

The random variables $\{\xi_j(n)\}$ are independent, identically-distributed, complex Gaussian variables. They may be expressed as

$$\xi_j(n) = \xi_j^{(1)}(n) + i\xi_j^{(2)}(n) \quad , \quad n=0,1,\dots \quad (C.4)$$

where $\xi_j^{(1)}(n)$ and $\xi_j^{(2)}(n)$ are, respectively, the real and imaginary parts of $\xi_j(n)$. For each n the variables $\xi_j^{(1)}(n)$ and $\xi_j^{(2)}(n)$ are independent, zero-mean, unit variance, real Gaussian variables, and both components of $\xi_j(n)$ are independent of each other for all values of n .

To generate $\tilde{G}_j(nT_0)$ directly using the convolution (C.2), we would have to approximate the infinite summation with a sufficiently accurate truncated summation. Because $\sigma_j T_0$ is very small, the length of this truncated summation would be large and we would expect error accumulation and an attendant loss of accuracy. However, our particular choice of an approximating correlation function (C.1) allows us to generate the random sequence $G_j(nT_0)$ iteratively. This was, of course, the primary consideration in selecting this particular approximation. The iterative scheme is given below

$$\begin{aligned} \tilde{G}_j(nT_0 + 3T_0) = & K_j \exp[-2\pi\rho\sigma_j T_0 + 2\pi i\nu_j(n+3)T_0] \xi_j(n+2) \\ & + K_j \exp[-4\pi\rho\sigma_j T_0 + 2\pi i\nu_j(n+3)T_0] \xi_j(n+1) \\ & + \exp[-6\pi\rho\sigma_j T_0 + 6\pi i\nu_j T_0] \tilde{G}_j(nT_0) \\ & - 3 \exp[-4\pi\rho\sigma_j T_0 + 4\pi i\nu_j T_0] \tilde{G}_j(nT_0 + T_0) \\ & + 3 \exp[-2\pi\rho\sigma_j T_0 + 2\pi i\nu_j T_0] \tilde{G}_j(nT_0 + 2T_0) \end{aligned} \quad (C.5)$$

$$\begin{aligned} n & \geq 0 \\ j & = 1, \dots, N \end{aligned}$$

where

$$K_j = \frac{2}{\sqrt{3}} A_j (2\pi\rho\sigma_j T_0)^{5/2}, \quad j=1, \dots, N \quad (C.6)$$

and, as discussed earlier, we will choose $\rho = 2.1$. To start this iteration we need $\tilde{G}_j(0)$, $\tilde{G}_j(T_0)$ and $\tilde{G}_j(2T_0)$ given by

$$\tilde{G}_j(0) = A_j W_j(1) \quad (C.7)$$

$$\tilde{G}_j(T_0) = \exp[2\pi i v_j T_0] \cdot \gamma_j(1) W_j(2) + \lambda_j(1) \tilde{G}_j(0) \quad (C.8)$$

$$\begin{aligned} \tilde{G}_j(2T_0) = \exp[4\pi i v_j T_0] \cdot \{ & \gamma_j(2) W_j(3) + K_j \exp[-2\pi\rho\sigma_j T_0] \xi_j(1) \\ & + \lambda_j(1) [1 - \lambda_j(2)] \tilde{G}_j(T_0) + \lambda_j(2) \tilde{G}_j(0) \} \end{aligned} \quad (C.9)$$

$$j=1, \dots, N.$$

Here $W_j(1)$, $W_j(2)$, $W_j(3)$, and $\xi_j(1)$ are independent, complex, Gaussian variables whose real and imaginary parts are independent and have zero mean and unit variance. The other terms appearing in (C.7)-(C.9) are

$$\lambda_j(1) = [1 + (4\pi\rho\sigma_j T_0) + \frac{1}{3} (4\pi\rho\sigma_j T_0)^2] \cdot \exp[-4\pi\rho\sigma_j T_0] \quad (C.10)$$

$$\lambda_j(2) = [1 + (8\pi\rho\sigma_j T_0) + \frac{1}{3} (8\pi\rho\sigma_j T_0)^2] \cdot \exp[-8\pi\rho\sigma_j T_0] \quad (C.11)$$

$$\gamma_j(1) = A_j [1 - \lambda_j^2(1)]^{1/2} \quad (C.12)$$

$$\gamma_j(2) = A_j \left[\left(1 - \lambda_j^2(1)\right) \left(1 - \lambda_j^2(2)\right) - \frac{4}{3} \left(2\pi\rho\sigma_j T_0\right)^5 \exp[-4\pi\rho\sigma_j T_0] \right]^{1/2} \quad (C.13)$$

The coefficients A_j are determined by the attenuation of each return via Eqn. (43).

It remains to generate the sequence of independent, Gaussian variables $\{\xi_j(n)\}$. We begin by using the congruence method to generate a sequence of uniform random variables. This method generates a sequence of random integers via the iterative scheme [24]

$$Y_{n+1} = a \cdot Y_n \pmod{M} . \quad (C.14)$$

For the quantities a and M , we have found $a = 7^5$ and $M = 2^{31}$ to be effective. Multiplication is done using double precision arithmetic but the final result is expressed as a single precision variable. Upon division of $\{Y_n\}$ by 2^{31} a sequence of independent, uniform $[0,1]$ variables is produced. This sequence is then transformed into a sequence of independent, complex, Gaussian variables. If u_1 and u_2 are real, independent, uniform variables, the real and imaginary parts of the variable ξ defined by

$$\xi = (-2 \ln u_1)^{1/2} \exp[2\pi i u_2] \quad (C.15)$$

are independent and Gaussian with zero mean and unit variance [24]. Thus, we obtain the desired sequence of complex Gaussian variables for use as the filter input in Eqn. (C.5).

APPENDIX D
SIGNAL ANALYSIS PROGRAM


```

C      # 61 PATH LENGTH (KM)
C      # 71 DELAY AT CARRIER FREQUENCY (SEC.)
C      # 81 RECEIVED CARRIER PHASE (CYCLES)
C      # 91 SIGNAL DELAY (SEC.)
C      #101 AMPLITUDE DISTORTION (SEC/MHZ)
C      #111 PHASE DISTORTION (SEC/MHZ**2)
C      #121 ATTENUATION (DB)
C      #131 DOPPLER SHIFT (HZ)
C      #141 DOPPLER SPREAD (HZ)
C      WARNING: NPATH MUST NOT EXCEED 10
C      WARNING: NCONV MUST NOT EXCEED 400 (HOWEVER, SEE WARNING IN
C      SUBROUTINE 'IMPULS').
C      WARNING: NPRINT MUST NOT EXCEED 10*000

      A1=(0.,1.)
      PI=3.14159265359
      ALPHA=2.1
      INTF='SITE'
      INITIALIZE VARIABLES AND ARRAYS FOR SUBROUTINE 'GAIN'
      NCALL=0
      ISFID=7**5
      DUTOT=1.10
      Y1=(0.,0.)
      DUTJ=17
      C(I,J)=URLE(0.)
      CONTINUE
      DUA=1.4
      X(I)=J*(0.20.)
      CONTINUE
      10 CONTINUE
      END INPUT DATA
      READ(F,B,M,R,ANG,L,NPATH)
      READ(S,YOJ,TIME)
      READ(G,DELAY,BATTEN)
      READ(M,CONV)
      READ(N,MIN)
      READ(N,GAIN)
      READ(P,PRINT)
      READ(A,NAIPE)
      DOPUT=1+NPATH
      READ(S,Y455)(I(I,J),J=1,I)
      READ(S,Y56)(I(I,J),J=1,I)
      READ(S,Y57)(I(I,J),J=1,I)
      CONTINUE
      20 CONTINUE
      END READ INPUT DATA
      DETERMINE IF LIMITS FOR NPATH, NCONV OR NPRINT ARE EXCEEDED
      IF(NPATH=10)??Z2Z21
      21 WRITE(6,901)
      GOTO999
      22 IF(NCONV=400)Z6Z6*24
      24 WRITE(6,902)
      26 IF(NPRINT=1000)Z8Z8*27
      27 WRITE(6,905)
      GOTO999
      END DETERMINATION OF EXCEEDED LIMITS
      THE SAMPLE INTERVAL TO IS HALF THE NYQUIST SAMPLE INTERVAL
      28 TO=1./(.34*2000.)

```

```

C      INITIAL ARRAY ARRAYS FOR CONVOLUTION
      DUBUT=1,NPATH
      D2(1)=1,10,2,2,PI*(RM*2)
      D3(1)=1,1,1,1,2,2,PI*(RM*3)*(16*03)
      NM=ABS(T(1,0))/10
      XM=10-10*FLOAT(NM)
      IF(T(1,0))32,39,34
32     NM2=-1
      GOTO36
34     NM2=1
36     IF(NM)5,33,36,39
38     NIC(1)=1,NN2
      GOTO40
39     NIC(1)=4,NI+1,NN2
40     CUNTINUL
C      END INITIALIZATION OF ARRAYS FOR CONVOLUTION
C      DETERMINE NOMB
      NG1=GOENAY/10
      XS=10-10*FLOAT(NG1)
      IF(XG1)5,42,42,44
42     NGND=NG1
      GOTO45
44     NGND=NG1+1
C      END DETERMINATION OF NGND
C      DETERMINE MAX. AND MIN. DELAY SHIFT PARAMETERS
45     LLIMIT=NCINVL+1
      NIMAX=NGND
      NIMIN=NGND
      DUBOT=1,NPATH
      NIMAX=XO(NIMAX,MIT)
      NIMIN=XO(NIMIN,MACI)
48     CUNTINUL
C      END DETERMINATION OF MAX. AND MIN. SHIFT PARAMETERS
C      READ INITIAL INPUT SEQUENCE
      MHEAD=NIMAX-NIMIN+LLIMIT
      MFEAD1=READ-1
      TF(NREAD)=5000150+50.55
      MFI(16,903)
      GOTO999
50     DUBUL=1,READ
      XLL=FLJAT(L-1)
      READ(10,904)SIGIN(L)
60     CUNTINUL
C      END READ INITIAL INPUT SEQUENCE
      MSHIFTE=
      CALL IMPULS(NCONV,NPATH,0,0,0,0)
C      DUBOON=1,NUMIN
C      DETERMINE DISTORTED THERMOSPHERE RETURNS
      DUBOT=1,NPATH
      RCT=(0,0,0)
70     CUNTINUL
      DUBOOL=1,LLIMIT
      LUM2=NCUNVLL+2
      LSEL=NCUNVLL+NSHIFT+1
      DUBUT=1,NPATH
      LSEL=NI(1)
      00 200 IS THE FUNDAMENTAL LOOP FOR DETERMINING THE OUTPUT
      FOR EACH INDER M (N CORRESPONDS TO AN ARGUMENT OF (N-1)*10).

```



```

WRITE(6,920)NMIN
7F(NGA1,203,203,204
203 WRITE(6,921)
204 WRITE(6,922)LLIMIT
WRITE(6,923)NMIN,NIMAX
WRITE(6,924)
WRITE(6,925)GUELAY,RATTEN
WRITE(6,926)
WRITE(6,927)
WRITE(6,928)
WRITE(6,929)
WRITE(6,930)
DUPOA1=L*PATH
IN=(1,1),1.E*05
WRITE(6,931)IN,(1,2),(1,3),(1,4),(1,5),(1,6),(1,7),(1,8),(1,9),(1,10),(1,11),(1,12),(1,13),(1,14)
206 CONTINUE
WRITE(6,930)
WRITE(6,924)
WRITE(6,930)
PRINT OUTPUT ARRAY = PRTOUT(N)
WRITE(6,906)
NIPRNT=LNAT(NPRIN)/3.
DUZ10L=L*ANLPR
LA=3*(L-1)+1
L=LA+1
L=LA+2
WRITE(6,907)LA,PRTOUT(LA),L,PRTOUT(LB),L,C,PRTOUT(LC)
210 CONTINUE
C
C ENU PRINTING OF OUTPUT DATA SUMMARY AND OUTPUT ARRAY
900 FORMAT(46)
901 FORMAT(1X,'PATH IS GREATER THAN 100 THIS EXCEEDS THE ALLOCATED AR
RAY STORAGE. PROGRAM IS TERMINATED.')
902 FORMAT(1X,'COUNT IS GREATER THAN 400 THIS EXCEEDS THE ALLOCATED
ARRAY STORAGE. PROGRAM IS TERMINATED.')
903 FORMAT(1X,'THE ARRAY STORAGE REQUIREMENTS FOR SIGIN(L) HAVE BEEN
EXCEEDED. PROGRAM IS TERMINATED.')
904 FORMAT(2E13,4)
905 FORMAT(1X,'THE ARRAY STORAGE REQUIREMENTS FOR PRTOUT(N) HAVE BEEN
EXCEEDED. PROGRAM IS TERMINATED.')
906 FORMAT(5X,'INDEX',10X,'OUTPUT',17X,'INDEX
1',10X,'OUTPUT'//)
907 FORMAT(2X,16,2X,2E13,6,4X,16,2X,2E13,6)
910 FORMAT(33X,'OUTPUT DATA SUMMARY'//)
911 FORMAT(1X,'IONOSPHERE TRANSMITTER=RECEIVER PARAMETERS'//)
912 FORMAT(10X,'DAYTIME ELECTRON DENSITY PROFILE')
913 FORMAT(10X,'NIGHTTIME ELECTRON DENSITY PROFILE')
914 FORMAT(10X,'DISTANCE BETWEEN TRANSMITTER AND RECEIVER =',F8.2,' K
IM.')
915 FORMAT(10X,'CARRIER FREQ. =',F7.3,' MHz. BANDWIDTH =',F7.2,' K
Hz.')
917 FORMAT(1X,'SIGNAL ANALYSIS PARAMETERS'//)
918 FORMAT(10X,'TIME SAMPLING INTERVAL=TOP EQUALS',F10.3,' SEC. (THIS
IS HALF THE MINUTEST SAMPLING INTERVAL)')
920 FORMAT(10X,'THE LENGTH OF THE INPUT SEQUENCE IS',I4)
921 FORMAT(10X,'THE GAINS FOR THE IONOSPHERE RETURNS ARE SET = 1 (THEY
ARE NONRANDOM)')
922 FORMAT(10X,'THE IONOSPHERE IMPULSE RESPONSE IS IRRUCATED TO',I4,'
SAMPLES')
923 FORMAT(10X,'MINIMUM DELAY SHIFT =',I4,3X,'MAXIMUM DELAY SHIFT =',
I4,4)

```

```

924 FORMAT(1X,'THE FOLLOWING DATA REPRESENTS THE RECEIVED, COMPLEX GAS
    IEBAND SIGNAL. IT INCLUDES THE GROUNDWAVE AND ALL IONOSPHERE RETURN
    2S//')
930 FORMAT(1X)
934 FORMAT(1X,'COMPUTER CHANNEL PARAMETERS//')
935 FORMAT(1X,'GROUNDWAVE DELAY =',F10.3,' SEC. ATTENUATION =',
    1,'F10.3,' DB.')
936 FORMAT(1X,'IONOSPHERE RETURN//')
938 FORMAT(1X,'MODE',3X,'SOLUTION',3X,'RAY ANGLE',F3.1,' DEG',3X,'CARRI
    IER',3X,'CARRIER',3X,' SIGNAL',3X,'AMPLITUDE',3X,'PHASE',5X,'ATT
    ZENITHION',2X,'DOPPLER',4X,'DOPPLER')
939 FORMAT(10X,'INDICATION',2X,'(DEGREES)',2X,'LENGTH',3X,'DELAY',6X,'P
    IASE',6X,'DELAY',3X,'DISTORTION',1X,'DISTORTION',3X,'(DB)',7X,'S
    HIFT',5X,'SPREAD')
940 FORMAT(9X,'(UNNU SOLN)',13X,'(KN)',3X,'(SEC)',3X,'(CYCLES)',5X,'(C
    ISEC)',4X,'(SEC/MHZ)',1X,'(SEC/MHZ**2)',15X,'(MHZ)',7X,'(MHZ)')
951 FORMAT(1X,'1',A2,'X',A4,'A',A1,'A',A4,'F5.2',1X,'F9.2',1X,'E10.3',
    1,'E10.3',1X,'E10.3',2X,'E10.3',1X,'E10.3',1X,'E10.3')
955 FORMAT(11,'A2',A4,'A',A4,'E16.9')
956 FORMAT(4E16.9)
957 FORMAT(3E16.9)
999 STOP
    END
0021023013 IS THE LOCATION FOR EXCEPTIONAL ACTION ON THE I/O STATEMENT AT 00210050
0021023015 IS THE LOCATION FOR EXCEPTIONAL ACTION ON THE I/O STATEMENT AT 00210055
0021023011 IS THE LOCATION FOR EXCEPTIONAL ACTION ON THE I/O STATEMENT AT 00210050
0021023013 IS THE LOCATION FOR EXCEPTIONAL ACTION ON THE I/O STATEMENT AT 00210045
0021023015 IS THE LOCATION FOR EXCEPTIONAL ACTION ON THE I/O STATEMENT AT 00210030
0021023011 IS THE LOCATION FOR EXCEPTIONAL ACTION ON THE I/O STATEMENT AT 00210033
0021023013 IS THE LOCATION FOR EXCEPTIONAL ACTION ON THE I/O STATEMENT AT 00210015
    SEGMENT 002 IS 0288 LONG

```

START OF SEGMENT 009

```

SUBROUTINE IMPULS(MCONVLS,NPATH,DZ,D3,D0)
DIMENSION DZ(10),D3(10)
COMPLEX D(10000),XI(9),XIO,AI
C
C SUBROUTINE COMPUTES MFLAY DISTORTION IMPULSE RESPONSES FOR
C EACH IONOSPHERE RETURN
C
C MCONVLS = LENGTH OF TRUNCATED IMPULSE RESPONSE (MAX. 400)
C NPATH = NUMBER OF RETAINED IONOSPHERE RETURNS
C DZ(1) = ARRAY OF AMPLITUDE DISTORTION COEFFICIENTS
C D3(1) = ARRAY OF PHASE DISTORTION COEFFICIENTS
C
C SUBROUTINE RETURNS ARRAY D(I,N), I DESIGNATES THE PARTICULAR
C IONOSPHERE RETURN, N DESIGNATES THE ARGUMENT OF THE IMPULSE
C RESPONSE. N=1 CORRESPONDS TO AN ARGUMENT OF -MCONVLS*10)
C N=2-MCONVLS+1 CORRESPONDS TO AN ARGUMENT OF -MCONVLS*10.
C
C WARNING: THE MAXIMUM ERROR IN THE FRESNEL INTEGRAL (FROM
C SUBROUTINE FRSHML) IS 1.0 E-09, AS A CONSEQUENCE
C OF THE ITERATIVE METHOD USED TO EVALUATE D(I,N) BREAKS
C DOWN WHEN N EXCEEDS APPROXIMATELY 25. FOR THIS
C REASON IT IS NOT ADVISED TO CHOOSE MCONVLS LARGER
C THAN 25.
C
PI=3.14159265359
AI=(0.,1.)
NLIMIT=MCONVLS+1
D(1)=1./NPATH
D(2)=D(1)
D(3)=D(1)
D(4)=D(1)
D(5)=D(1)
ARG=FLOAT(N-1)*MCONVLS*PI
IF(DD2)30,5,30
5 IF(ARG)10,6,10
6 XI(1)=(COS(0.))
XI(2)=(2./3.)*S(1./3.)
XI(3)=(COS(0.))
XI(4)=(COS(0.))
XI(5)=(4./5.)
XI(6)=(2./7.)*S(1./7.)
XI(7)=(COS(0.))
XI(8)=(2./9.)*S(1./9.)
XI(9)=(COS(0.))
GOTO 85
10 XI(10)=(2./10.)*S(1./10.)/ARG)
XI(11)=-2.*AI*(COS(ARG)+S(INC(ARG)/ARG))/ARG
D(20)=2.*9
KI=K-1
XI(K)=(-AI*(ARG))+(C*EXP(AI*ARG))-(C*1.)*EXP(LOAT(K))*C*EXP(-AI*ARG))+FL
10 AT(K)*S(K*PI)
20 CONTINUE
GOTO 85
30 ARG=ARG
D(20)=DD2
CALL FRSHML(DDU2,AARG,XIO)
XI(1)=(-S(INC(ARG))*C*EXP(-AT*DD2))+5*ARG*XIO)/DD2
XI(2)=(AI*(COS(ARG)))-C*EXP(-AT*DD2))+5*ARG*XI(1)-AI*5*XIO)/DD2
N(40)=K-9

```

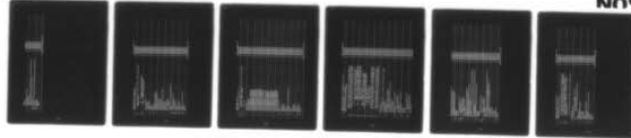
AD-A054 726

SYSTEMS EXPLORATION INC SAN DIEGO CA
HF CHANNEL SIMULATOR FOR WIDEBAND SIGNALS. A
MAR 78 R LUGANNANI, H C BOOKER, L E HOFF
NOSC-TR-208

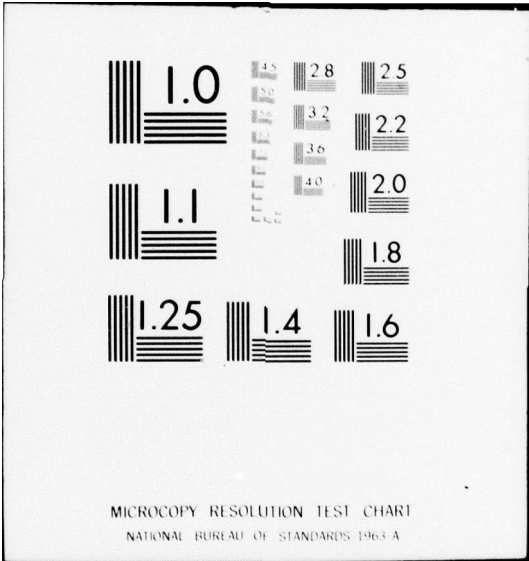
F/G 17/2
MATHEMATICAL MODEL--ETC(U)
N00123-76-C-1090

UNCLASSIFIED

2 of 2
AD
A054726



END
DATE
FILMED
7-78
DDC



```

K1=N-1
K2=N+2
KI=(FLOAT(K1/2)+1.E-06
XINDC=ZKNT
XINDC01=XIND
XI(K)=1./2.*SDD2))+(2.*AI*EXP(-AI*P02))+(XINDC-COS(ARG))*AI*XINDC*S
1(INCARG)))*ARG*X1(K1)-AI*FLOAT(K1)*XI(K2)
40 CONTINUE
45 D1(EW)=5*(X10-AI*DD3)*XI(K3)+5*(DD3+2)*XI(K4)+AI*(1./EA)*S(DD3+2)*
XI(K5)
50 CONTINUE
100 CONTINUE
RETURN
END

```

```

C 009100B210
C 009100B312
C 009100B415
C 009100B715
C 009100B914
C 009100BA15
C 009100B912
C 009100AA10
C 009100CA11
C 009100C413
C 009100CB15
C 009100CC10
C 009100D411
C 009100DD14

```

SEGMENT 009 IS ODD LUNG

M
-C